Subscriber access provided by American Chemical Society

Organometallic nitrosyl chemistry. 43. Synthesis, characterization, and physical properties of unusual cyclopentadienyl bis(benzyl) nitrosyl complexes of molybdenum and tungsten

Peter. Legzdins, Everett C. Phillips, James. Trotter, Vivien
C. Yee, Frederick W. B. Einstein, and Richard H.. Jones

Organometallics, **1991**, 10 (4), 986-1002• DOI: 10.1021/om00050a034 • Publication Date (Web): 01 May 2002

Downloaded from http://pubs.acs.org on March 8, 2009

More About This Article

The permalink http://dx.doi.org/10.1021/om00050a034 provides access to:

- Links to articles and content related to this article
- Copyright permission to reproduce figures and/or text from this article

ACS Publications
High quality. High impact.

Organometallics is published by the American Chemical Society. 1155 Sixteenth Street
N.W., Washington, DC 20036

986 *Organometallics* 1991, *10*, 986–1002

Synthesis, Characterization, and Physical Properties of Unusual Cyclopentadienyl Bis(benzyl) Nitrosyl Complexes of Molybdenum and Tungsten[1,2]

Peter Legzdins,[*,†] Richard H. Jones,[‡] Everett C. Phillips,[†] Vivien C. Yee,[†] James Trotter,[*,†] and Frederick W. B. Einstein[*,‡]

Departments of Chemistry, The University of British Columbia, Vancouver, British Columbia, Canada V6T 1Y6, and Simon Fraser University, Burnaby, British Columbia, Canada V5A 1S6

Received October 3, 1990

Treatment of either the dichloro or diiodo nitrosyl precursors Cp′M(NO)X_2 (Cp′ = Cp (η^5-C_5H_5) or Cp* (η^5-C_5Me_5); M = Mo or W; X = Cl or I) in THF/Et_2O with 2 equiv of a benzyl Grignard reagent, Ph′CH_2MgCl (Ph′ = C_6H_5 or 2,4,6-$Me_3C_6H_2$), at 0 °C affords the corresponding bis(benzyl) nitrosyl complexes, Cp′M(NO)(CH_2Ph′)$_2$, isolated yields typically being 50–65%. All the bis(benzyl) nitrosyl complexes are relatively high melting (143–163 °C), orange-red, diamagnetic solids that are soluble in most common organic solvents. They are all stable to air in the solid state for at least 2 months, and only solutions of the tungsten species react with O_2 to produce moderate yields of the corresponding dioxo benzyl complexes, Cp′W(O)$_2$(CH_2Ph′). The spectroscopic properties of the bis(benzyl) complexes are consistent with their possessing 18-electron, monomeric Cp′M(NO)(η^1-CH_2Ph′)(η^2-CH_2Ph′) molecular structures. Variable-temperature ^1H and $^{13}C\{^1H\}$ NMR spectra of all the compounds in CD_2Cl_2 establish that they are stereochemically nonrigid in solutions at ambient temperatures, the principal fluxionality involving the two benzyl ligands exchanging their modes of attachment to the metal centers. ^{13}C NMR spectroscopy also establishes that the low-temperature limiting structures of the complexes in solution are identical with their solid-state molecular structures. Interestingly, the tungsten bis(benzyl) complexes exhibit the more facile fluxional processes in solution, this increased nonrigidity apparently rendering the tungsten complexes more reactive to Lewis bases. Crystal structure analyses of the five bis(benzyl) nitrosyl complexes have been performed in order to establish their solid-state molecular structures. Crystals of CpMo(NO)(CH_2Ph)$_2$ (**1a**) are orthorhombic, *Pbca*, with a = 10.122 (1) Å, b = 15.625 (2) Å, c = 20.770 (2) Å, and Z = 8; the structure was solved by conventional heavy-atom methods and was refined by full-matrix least-squares procedures to R = 0.024 and R_w = 0.031 for 2057 absorption-corrected reflections with $I > 3\sigma(I)$. Crystals of CpMo(NO)(2,4,6-$Me_3CH_2C_6H_2$)$_2$ (**1b**) are triclinic, $P\bar{1}$, with a = 9.4113 (19) Å, b = 8.3499 (18) Å, c = 15.4533 (18) Å, α = 98.004 (18)°, β = 100.408 (15)°, γ = 110.511 (16)°, and Z = 2; R = 0.031 and R_w = 0.039 for 3983 reflections. Crystals of Cp*Mo(NO)(CH_2Ph)$_2$ (**2**) are monoclinic, $P2_1/c$, with a = 13.969 (5) Å, b = 16.125 (3) Å, c = 9.778 (5) Å, β = 110.67 (4)°, and Z = 4; R = 0.029 and R_w = 0.038 for 2775 reflections. Crystals of CpW(NO)(CH_2Ph)$_2$ (**3**) are orthorhombic, *Pbca*, with a = 10.110 (1) Å, b = 15.614 (2) Å, c = 20.654 (2) Å, and Z = 8; R = 0.025 and R_w = 0.028 for 2192 reflections. Crystals of Cp*W(NO)(CH_2Ph)$_2$ (**4**) are monoclinic, $P2_1/c$, with a = 13.916 (4) Å, b = 16.101 (3) Å, c = 9.757 (3) Å, β = 110.08 (2)°, and Z = 4; R = 0.021 and R_w = 0.030 for 3471 reflections. All the complexes are monomeric and possess distinctive Cp′M(NO)(η^1-CH_2Ph′)(η^2-CH_2Ph′) four-legged piano-stool molecular structures in the solid state. The most chemically interesting feature of each structure involves the η^2-benzyl ligand, which is characterized by the following six distinctive parameters: (a) its M–CH_2 bond length is significantly shorter (i.e. by 0.04–0.06 Å) than that involving the η^1-CH_2Ph′ group; (b) its CH_2–C_{ipso} bond length is also significantly shorter than that seen for the η^1-CH_2Ph′ group; for instance, C(11)–C(12) = 1.445 (6) and 1.457 (6) Å and C(21)–C(22) = 1.472 (4) and 1.497 (5) Å in complexes **1a** and **2**, respectively; (c) its M–C_{ipso} distance (ranging between 2.433 (3) and 2.510 (4) Å) is well within the range expected for a normal group 6 metal–carbon single bond; (d) its angle at the methylene carbon atom (i.e. C(12)–C(11)–M) is well below the value expected for a tetrahedral sp^3-carbon environment, being typically in the range 81–85°; (e) its two M–C_{ortho} distances (ranging between 2.81 and 3.26 Å) are longer than the range commonly observed for strong group 6 M–C single bonds; and (f) its four phenyl C–C distances from C(13) to C(17) are essentially identical, and the observed bond lengths of approximately 1.38 Å suggest the presence of delocalized multiple bonding extending over these carbons. These metrical parameters indicate that the η^2-benzyl groups may be viewed to function as formal three-electron ligands via C–M σ bonds involving their methylene and ipso carbon atoms. This bonding rationale is also consistent with the physical properties exhibited by the bis(benzyl) nitrosyl complexes.

Introduction

Transition-metal alkyl complexes are commonly invoked as intermediates in many important stoichiometric and catalytic processes.[3] However, the stabilities and reactivities of these complexes are often markedly influenced by the natures of both the metal and the other ligands present in the complex.[3] In this latter regard, relatively little is known at present about how the physical and chemical properties of transition-metal–carbon σ bonds are affected by the presence of nitrosyl ligands in the metal's coordination sphere.[4] Our recent research efforts have thus been directed at ascertaining the effects exerted by Cp′M(NO) groups [Cp′ = Cp (η^5-C_5H_5) or Cp* (η^5-C_5Me_5); M = Mo or W] on their ancillary hydrocarbon ligands. Specifically, we have to date demonstrated that the Cp′Mo(NO) fragments prefer to bind acyclic, conjugated dienes in a twisted, transoidal fashion, an unprecedented

---

[†] The University of British Columbia.

[‡] Simon Fraser University.

(1) Organometallic Nitrosyl Chemistry. 43. Part 42: Dryden, N. H.; Legzdins, P.; Phillips, E. C.; Trotter, J.; Yee, V. C. *Organometallics* **1990**, *9*, 882.

(2) Taken in part from: Phillips, E. C. Ph.D. Dissertation, The University of British Columbia, 1989. Yee, V. C. Ph.D. Dissertation, The University of British Columbia, 1990.

(3) Collman, J. P.; Hegedus, L. S.; Norton, J. R.; Finke, R. G. *Principles and Applications of Organotransition Metal Chemistry*; University Science Books: Mill Valley, CA, 1987.

(4) Richter-Addo, G. B.; Legzdins, P. *Chem. Rev.* **1988**, *88*, 991.

0276-7333/91/2310-0986$02.50/0 © 1991 American Chemical Society

feature that leads to the bound dienes exhibiting novel reactivities toward representative nucleophiles and electrophiles.[5] Furthermore, we have also shown that the characteristic chemistry of thermally stable, 16-electron CpM(NO)(alkyl)$_2$ complexes is dominated by their ability to effect the initial coordination of a variety of small molecules to their metal centers.[6,7]

During much of our earlier work, the prototypal CpM(NO)(alkyl)$_2$ complex used was CpW(NO)(CH$_2$SiMe$_3$)$_2$ simply because it was easily preparable in high yields and its reactivity with various substrates could be conveniently monitored by conventional spectroscopic techniques.[6,7] However, as we began to extend our investigations to encompass a wider range of Cp′M(NO)(alkyl)$_2$ complexes, we soon discovered that the chemical properties of these species can also be markedly influenced by the natures of their alkyl ligands. For instance, we have recently reported that a large number of these molybdenum and tungsten dialkyl complexes react with molecular oxygen either rapidly in Et$_2$O solutions (1–6 h) or slowly in the solid state (1–2 days) to afford a novel series of dioxo alkyl complexes, Cp′M(O)$_2$R, in good yields:[8]

$$\mathrm{Cp'M(NO)R_2} + \mathrm{O_2} \longrightarrow \mathrm{CpM(O)_2R} + \text{"RNO"} \quad (1)$$

[Cp′ = Cp* or Cp; M = Mo, R = CH$_2$SiMe$_3$ or Me; M = W, R = CH$_2$SiMe$_3$, CH$_2$CMe$_3$, CH$_2$CMe$_2$Ph, CH$_2$Ph or Me]

Proton NMR and ^{18}O$_2$-labeling studies are consistent with reactions 1 proceeding via initial attack of the dioxygen at the coordinatively unsaturated metal center:[8]

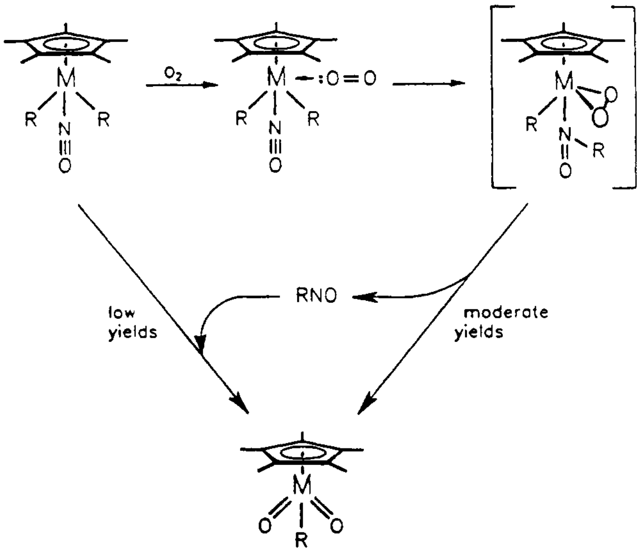

Interestingly, though, reaction of the molybdenum bis(benzyl) complex CpMo(NO)(CH$_2$C$_6$H$_5$)$_2$ with O$_2$ under identical experimental conditions does not generate the corresponding dioxo benzyl complex, CpMo(O)$_2$(CH$_2$C$_6$H$_5$). Furthermore, both CpM(NO)(CH$_2$Ph)$_2$ complexes (M = Mo or W) are considerably more stable in the solid state than are their dialkyl analogues (i.e. CpM(NO)R$_2$ with R = CH$_2$SiMe$_3$, CH$_2$CMe$_3$, and CH$_2$CMe$_2$Ph), remaining unchanged when exposed to air under ambient conditions for periods of 1–2 months.

With a view to gaining some insight as to why the bis(benzyl) complexes are relatively more inert to air than are their dialkyl analogues, we undertook a detailed investigation of a series of such Cp′M(NO)(CH$_2$Ph′)$_2$ complexes, namely those having Cp′ = Cp or Cp*, M = Mo or W, and Ph′ = Ph (C$_6$H$_5$) or 2,4,6-Me$_3$C$_6$H$_2$. This paper presents complete details of the synthesis, characterization, and some physical properties of these compounds, including the results of single-crystal X-ray crystallographic analyses of five of these complexes. Taken as a whole, this paper presents evidence which demonstrates clearly the effects that η^2-benzyl ligands, which function as formal three-electron donors to the metal centers, can have on the physical and chemical properties of these compounds.

Experimental Section

All reactions and subsequent manipulations involving organometallic reagents were performed under anhydrous and anaerobic conditions using conventional Schlenk-tube techniques under an atmosphere of dinitrogen or argon.[9,10] All solvents were purchased from BDH Chemicals and were dried according to conventional procedures.[11] All solvents were freshly distilled and deaerated with dinitrogen for approximately 10 min just prior to use. The benzyl chloride (PhCH$_2$Cl) reagent was purchased from Aldrich Chemical Co. and was dried over MgSO$_4$ before use. The related organic compound α^2-chloroisodurene (2,4,6-Me$_3$C$_6$H$_2$CH$_2$Cl) was also obtained from Aldrich and was purified by vacuum distillation. The Grignard reagents, PhCH$_2$MgCl and 2,4,6-Me$_3$C$_6$H$_2$CH$_2$MgCl, were prepared by employing well-established procedures.[12] The methanol and *tert*-butyl alcohol reagents were distilled from CaH$_2$ and stored over 3-Å molecular sieves prior to use.

The CpM(NO)I$_2$ complexes[13] (M = Mo,[16] W[17]) and Cp*W(NO)I$_2$[14a] were prepared by the appropriate literature methods. The complex Cp*Mo(NO)I$_2$ was prepared by treatment of Cp*Mo(NO)(CO)$_2$ with I$_2$ in a manner similar to that employed for the synthesis of its perhydro analogue.[18] The requisite Cp′M(NO)Cl$_2$ complexes (Cp′ = Cp, Cp*; M = Mo, W) were synthesized by treating the appropriate Cp′M(NO)(CO)$_2$ precursor complex with an equimolar amount of PCl$_5$ in Et$_2$O.[14c] The purity of the above reagents was established by elemental analysis before they were used. All other chemical reagents either were purchased from commercial suppliers or were prepared by published procedures.

Infrared spectra were recorded on a Nicolet 5DX FT-IR in-

---

(5) (a) Christensen, N. J.; Hunter, A. D.; Legzdins, P. *Organometallics* **1989**, *8*, 930. (b) Christensen, N. J.; Legzdins, P. Manuscript in preparation.

(6) Legzdins, P.; Martin, J. T.; Einstein, F. W. B.; Jones, R. H. *Organometallics* **1987**, *6*, 1826.

(7) Legzdins, P.; Rettig, S. J.; Sánchez, L. *Organometallics* **1988**, *7*, 2394.

(8) Legzdins, P.; Phillips, E. C.; Sánchez, L. *Organometallics* **1989**, *8*, 940.

(9) Shriver, D. F.; Drezdzon, M. A. *The Manipulation of Air-Sensitive Compounds*, 2nd ed.; Wiley-Interscience: Toronto, 1986.

(10) Wayda, A. L.; Darensbourg, M. Y. *Experimental Organometallic Chemistry: A Practicum in Synthesis and Characterization*; ACS Symposium Series 357; American Chemical Society: Washington, DC, 1987.

(11) Perrin, D. D.; Armarego, W. L. F.; Perrin, D. R. *Purification of Laboratory Chemicals*, 2nd ed.; Pergamon Press: Oxford, U.K., 1980.

(12) (a) Kharasch, M. S. *Grignard Reactions of Non-Metallic Substances*; Prentice-Hall: New York, 1954. (b) Sommer, L. H.; Whitmore, F. C. *J. Am. Chem. Soc.* **1946**, *68*, 481.

(13) The dihalo nitrosyl complexes Cp′M(NO)X$_2$ (Cp′ = Cp or Cp*; M = Mo or W; X = Cl, Br, or I) possess either monomeric[14a] or halide-bridged dimeric[14b,c] molecular structures in the solid state. However, the physical and chemical properties of these compounds in solutions are most consistent with their existing as solvated monomers.[15] Consequently, in this paper they are represented exclusively by their monomeric formulas.

(14) (a) Dryden, N. H.; Einstein, F. W. B.; Jones, R. H.; Legzdins, P. *Can. J. Chem.* **1988**, *66*, 2100. (b) Gomez-Sal, P.; de Jesús, E.; Michiels, W.; Royo, P.; de Miguel, A. V.; Martinez-Carrera, S. *J. Chem. Soc., Dalton Trans.* **1990**, 2445. (c) Dryden, N. H.; Legzdins, P. Manuscript in preparation.

(15) Herring, F. G.; Legzdins, P.; Richter-Addo, G. B. *Organometallics* **1989**, *8*, 1485.

(16) Bray, J.; Kita, W. G.; McCleverty, J. A.; Seddon, D. *Inorg. Synth.* **1976**, *16*, 24.

(17) Legzdins, P.; Martin, D. T.; Nurse, C. R. *Inorg. Chem.* **1980**, *19*, 1560.

(18) Nurse, C. R. Ph.D. Dissertation, The University of British Columbia, 1983.

(19) Some of the spectroscopic data for this compound have been reported previously.[7]

Table I. Analytical and IR and Mass Spectral Data for the Bis(benzyl) Nitrosyl Complexes

complex	low-resolution mass spectral data,[a] m/z[b]	analytical data, %						IR data (ν_{NO}), cm^{-1}	
		C		H		N			
		calcd	found	calcd	found	calcd	found	Nujol	CH$_2$Cl$_2$
CpMo(NO)(CH$_2$Ph)$_2$ (**1a**)[c]	375	61.13	61.10	5.13	5.10	3.75	3.84	1601	1601
CpMo(NO)(CH$_2$C$_6$H$_2$Me$_3$)$_2$ (**1b**)	459	65.64	65.80	6.83	6.90	3.06	3.01	1572	1585
Cp*Mo(NO)(CH$_2$Ph)$_2$ (**2**)[d]	445	65.01	64.91	6.59	6.68	3.16	3.06	1580	1578
CpW(NO)(CH$_2$Ph)$_2$ (**3**)[d]	461	49.48	49.38	4.15	4.16	3.04	2.81	1570	1570
Cp*W(NO)(CH$_2$Ph)$_2$ (**4**)[d]	531	54.25	54.45	5.50	5.45	2.64	2.80	1566	1553

[a] Probe temperatures 100–150 °C. [b] [P$^+$]; assignments involve the most abundant naturally occurring isotopes in each species (e.g. ^{98}Mo, ^{184}W, etc.). [c] The ν_{NO} in the IR spectra of this complex as a Nujol mull, or KBr pellet, or in CH$_2$Cl$_2$ solution is difficult to assign because of two nearly equally intense absorptions at 1601 and 1587 cm^{-1} due to the nitrosyl ligand and the phenyl group. [d] In both the Nujol mull and CH$_2$Cl$_2$ solution IR spectra of this complex, the ν_{NO} absorption contains a shoulder at 1595 cm^{-1} attributable to vibrations in the phenyl ring.

strument internally calibrated with a He/Ne laser. All ^{1}H NMR spectra were obtained on a Varian Associates XL-300 or a Bruker WP-80 spectrometer with reference to the residual proton signal of the CD$_2$Cl$_2$ solvent employed. The ^{13}C NMR spectra were recorded at 75 or 25 MHz on the Varian Associates XL-300 spectrometer or the Bruker WP-80 spectrometer, respectively, with reference to the ^{13}C signal of the solvent employed. All ^{1}H and ^{13}C chemical shifts are reported in parts per million downfield from Me$_4$Si. The low-temperature ^{1}H and ^{13}C NMR spectra were obtained on the instruments listed above by using their standard cooling apparatus calibrated with MeOH. To avoid unnecessary heating of the samples during decoupling experiments, the low-power Waltz-16[20] broad-band proton-decoupling technique (^{13}C{^{1}H}) was used. The use of gated decoupling [{^{1}H} off during data acquisition (ca. 0.8 s) and on between acquisitions (ca. 1.6 s)] permitted the collection of proton-coupled ^{13}C NMR spectra with excellent signal-to-noise ratios and resolution in reasonable times (1–6 h). Standard Varian Attached Proton Test (APT) experiments allowed the collection of ^{13}C NMR spectra which distinguished –CH$_3$ and –CH type carbons from –C and –CH$_2$ carbons. In all such spectra recorded during this work, –C and –CH$_2$ carbon signals are plotted in the positive direction, while signals due to –CH$_3$ and –CH type carbons are plotted in the negative direction. Low-resolution mass spectra were recorded at 70 eV on an Atlas CH4B or a Kratos MS50 spectrometer by Dr. G. K. Eigendorf and the staff of the mass spectrometry laboratory of this department using the direct-insertion method. Elemental analyses were performed by Mr. P. Borda of this department. The melting point determinations were performed on a Gallenkamp melting point apparatus, and the temperatures reported are uncorrected.

Preparation of the Complexes CpMo(NO)(CH$_2$Ph)$_2$ (1a), CpMo(NO)(CH$_2$C$_6$H$_2$-2,4,6-Me$_3$)$_2$ (1b), Cp*Mo(NO)(CH$_2$Ph)$_2$ (2), CpW(NO)(CH$_2$Ph)$_2$ (3), and Cp*W(NO)(CH$_2$Ph)$_2$ (4). The syntheses of all these bis(benzyl) complexes involved the treatment of the appropriate Cp′M(NO)X$_2$ precursors[13] (Cp′ = Cp or Cp*; M = Mo or W; X = Cl or I) with slightly more than 2 equiv of PhCH$_2$MgCl or 2,4,6-Me$_3$C$_6$H$_2$CH$_2$MgCl at 0 °C. The synthesis of CpW(NO)(CH$_2$Ph)$_2$ from CpW(NO)I$_2$ in this manner has been previously reported from these laboratories.[7] All the other bis(benzyl) nitrosyl complexes may be prepared similarly from their diiodo precursors, but the dichloro precursor complexes lead to more convenient workup procedures. The preparation of Cp*Mo(NO)(CH$_2$Ph)$_2$ (**2**) is described below in detail as a representative example.

To a stirred, olive green solution of Cp*Mo(NO)Cl$_2$ (1.50 g, 4.50 mmol) in THF (200 mL) at 0 °C was added dropwise via an addition funnel an Et$_2$O solution (17.40 mL, 0.52 M, 9.04 mmol) of PhCH$_2$MgCl diluted with Et$_2$O (20 mL). The reaction mixture changed in color from yellow-green to dark red as the addition proceeded. After the addition of the Grignard reagent had been completed, the reaction mixture was stirred for an additional 0.5 h at room temperature, whereupon it was treated with 0.5 mL of deaerated H$_2$O added by syringe. This addition resulted in the formation of a sticky yellow-white precipitate, but the color of the supernatant solution did not change. The precipitate (presumably solvated MgCl$_2$) was removed by filtration of the resulting mixture through a column of Celite supported on a medium-porosity glass frit. The filtrate was taken to dryness in vacuo, and CH$_2$Cl$_2$ (30 mL) was then added. The resulting orange-red mixture was chromatographed on an alumina column (Fisher neutral, 80–200 mesh, activity 3, 6 × 3 cm) made up in hexanes using CH$_2$Cl$_2$ as eluant. The single orange-red band that developed was eluted from the column and collected, and the volume of the eluate was diminished to approximately 10 mL under reduced pressure. The addition of an equal volume of hexanes to the concentrate caused 0.69 g of orange-red Cp*Mo(NO)(CH$_2$Ph)$_2$ to crystallize slowly from solution at room temperature. These crystals were collected by filtration and dried under vacuum at ambient temperature. Concentration of the mother liquor and cooling the resulting solution to –20 °C overnight afforded an additional 0.63 g (66% total isolated yield) of the desired bis(benzyl) complex **2** (mp 152–155 °C).

In a similar manner, orange-red crystals (2.73 g, 50% yield) of CpMo(NO)(CH$_2$Ph)$_2$ (**1a**), mp 146–149 °C, were prepared from CpMo(NO)I$_2$ (6.50 g, 14.6 mmol) and PhCH$_2$MgCl (22.0 mL, 1.37 M, 30.0 mmol) at 0 °C in THF (150 mL).

Large red crystals (0.84 g, 48% yield) of CpMo(NO)(CH$_2$C$_6$H$_2$-2,4,6-Me$_3$)$_2$ (**1b**), mp 159–161 °C, were prepared similarly from CpMo(NO)Cl$_2$ (1.00 g, 3.82 mmol) and 2,4,6-Me$_3$C$_6$H$_2$CH$_2$MgCl (68.2 mL, 0.11 M, 7.6 mmol, diluted with 20 mL of Et$_2$O) in THF (200 mL) at 0 °C.

Similarly, 0.96 g (53% yield) of red crystals of CpW(NO)(CH$_2$Ph)$_2$ (**3**), mp 143–145 °C dec, were prepared from CpW(NO)Cl$_2$ (1.37 g, 3.91 mmol) and PhCH$_2$MgCl (15.1 mL, 0.52 M, 7.85 mmol) at 0 °C in a THF (150 mL) and Et$_2$O (25 mL) solvent mixture.

Finally, 1.22 g (64% yield) of red crystals of Cp*W(NO)(CH$_2$Ph)$_2$ (**4**), mp 160–163 °C dec, were prepared from Cp*W(NO)Cl$_2$ (1.50 g, 3.57 mmol) and PhCH$_2$MgCl (11.1 mL, 0.65 M, 7.21 mmol) at 0 °C in a THF/Et$_2$O (150 mL/25 mL, respectively) solvent mixture.

The analytical, mass spectral, IR, ^{1}H NMR, and ^{13}C NMR data for all the new bis(benzyl) complexes synthesized during this work are presented in Tables I and II.

Reactions of the Cp′M(NO)(CH$_2$Ph)$_2$ Complexes (1a, 2, 3, and 4) with O$_2$. All these reactions involved treatment of solutions of the bis(benzyl) complexes with an excess of dioxygen. The reactions of the tungsten complexes Cp′W(NO)(CH$_2$Ph)$_2$ (i.e. **3** and **4**) with molecular oxygen in Et$_2$O have been previously reported by us.[8] Low yields of the corresponding dioxo benzyl complexes, Cp′W(O)$_2$(CH$_2$Ph), were obtained from these reactions after prolonged reaction times. The reactions of dioxygen with the molybdenum analogues were effected in a similar manner, as outlined below for **1a**.

Analytically pure CpMo(NO)(CH$_2$Ph)$_2$ (**1a**, 0.56 g) was dissolved in THF (15 mL) at room temperature, and most of the dinitrogen atmosphere above the resulting orange-red solution was removed in vacuo. An excess of molecular oxygen was then introduced into the reaction vessel until a pressure of ca. 2 atm was attained. The reaction vessel was then sealed, and the reaction mixture was stirred at ambient temperature. No color change occurred within the first 6–12 h, but after 2 days the solution had developed a green coloration and a large amount of a green precipitate had deposited. No proton resonances were discernible in a ^{1}H NMR spectrum of the green residue in CD$_2$Cl$_2$. An IR spectrum of the green residue as a Nujol mull displayed many bands in the spectral region 650–980 cm^{-1} characteristic of M—O, M═O, and M—

---

[20] Shaka, A. J.; Keeler, J.; Freeman, R. *J. Magn. Reson.* **1983**, *53*, 313.

O—M vibrations.[21] A low-resolution mass spectrum of the green product showed no peaks above *m/z* 194.

Reactions of the $Cp'W(NO)(CH_2Ph)_2$ Complexes 3 and 4 with Alcohols. These reactions were performed in a similar manner. The dry and deaerated alcohol (MeOH or *t*-BuOH) was added by microsyringe to solutions of the appropriate tungsten bis(benzyl) complex, $Cp'W(NO)(CH_2Ph)_2$ (Cp′ = Cp or Cp*), in a deuterated solvent. The reactions that ensued were monitored over a period of time by both ^1H and ^{13}C NMR spectroscopy. The results of these investigations and the characterization data for the tungsten alkoxide product complexes are presented below.

(a) Reaction of $Cp^*W(NO)(CH_2Ph)_2$ (4) with MeOH. A CD_2Cl_2 solution of $Cp^*W(NO)(CH_2Ph)_2$ (0.060 g, 0.113 mmol) and MeOH (4.6 μL, 0.113 mmol) was sealed in an NMR tube under a slight vacuum. An initial ^1H NMR spectrum of the reaction mixture displayed only resonances attributable to the two reactants. The NMR tube was then heated to 45 °C. The reaction was extremely slow, its ^1H NMR spectrum after 3 weeks showing that approximately half of the $Cp^*W(NO)(CH_2Ph)_2$ starting material remained. The new ^1H resonances that had appeared and slowly increased in intensity in the interim could be attributed to $Cp^*W(NO)(OCH_3)(CH_2Ph)$ and free $PhCH_3$.

NMR data for $Cp^*W(NO)(OCH_3)(CH_2Ph)$ in CD_2Cl_2: 300 MHz ^1H NMR δ 7.32–6.8 (m, 5 H, *Ph*), 2.80 (d, 1 H, $^2J_{H_aH_b}$ = 11.0 Hz, CH_aH_bPh), 2.51 (d, 1 H, $^2J_{H_aH_b}$ = 11.0 Hz, CH_aH_bPh), 2.34 (s, 3 H, $W(OCH_3)$), 1.95 (s, 15 H, $C(CH_3)_5$); 75 MHz $^{13}C\{^1H\}$ NMR δ 163.5, 145.5, 129.3, 128.5, 123.8 (aromatic Ph *C*'s; quaternary Ph *C* of CH_2Ph group), 112.9 ($C(CH_3)_5$), 42.6 ($^1J_{CW}$ = 99.8 Hz, CH_2Ph), 21.5 ($W(OCH_3)$), 9.8 ($C(CH_3)_5$).

NMR data for $PhCH_3$ in CD_2Cl_2: ^1H NMR δ 7.2–6.8 (m, 5 H, *Ph*), 2.13 (s, 3 H, $C_6H_5CH_3$); $^{13}C\{^1H\}$ NMR δ 129.2, 128.1, 125.6 (aromatic Ph *C*'s), 21.5 ($C_6H_5CH_3$).

(b) Reaction of $CpW(NO)(CH_2Ph)_2$ (3) with *t*-BuOH. A CD_2Cl_2 solution of $CpW(NO)(CH_2Ph)_2$ (0.060 g, 0.13 mmol) and *t*-BuOH (24.7 μL, 0.26 mmol) was sealed in an NMR tube under a slight vacuum. An initial ^1H NMR spectrum displayed only proton resonances due to the two starting materials. The NMR tube was then maintained at 45 °C in an oil bath for 1 month, but the ^1H NMR spectrum of its contents remained unchanged.

X-ray Crystallographic Analyses of Complexes 1a, 2, 3, and 4. All the X-ray structure determinations of the bis(benzyl) nitrosyl complexes **1a**, **2**, **3**, and **4** were performed in a similar manner. A suitable X-ray-quality crystal of each complex was obtained by slow crystallizations from Et_2O solutions at −20 °C effected over several days. After preliminary photographic investigation, each crystal was mounted in a thin-walled glass capillary under N_2 and transferred to an Enraf-Nonius CAD4-F diffractometer equipped with graphite-monochromated Mo Kα radiation (λ = 0.71069 Å). The crystals of $Cp^*Mo(NO)(CH_2Ph)_2$ (**2**) and $Cp^*W(NO)(CH_2Ph)_2$ (**4**) were cooled to 208 and 211 K, respectively, by using a locally developed apparatus based on a commercial Enraf-Nonius system. Final unit-cell parameters for each complex were obtained by least-squares analysis of $2(\sin\theta)/\lambda$ values for 25 well-centered high-angle reflections. The intensities of two standard reflections were measured every 5400 s of X-ray exposure time during the data collection of **1a** and showed no appreciable variation with time (<0.82%). Similarly, the intensities of three standard reflections were measured every hour during the data collection of complexes **2**, **3**, and **4**. For the crystals of **2** and **3** there appeared to be no appreciable variations in the intensities with time (<1.58% and <1.04%, respectively). However, some variations in the intensities of the three standard reflections over time were noted during the data collection for complex **4**. We believe that these latter variations were due to a periodic passage of liquid nitrogen through a glass transfer line onto the crystal. In all cases, however, the standard reflections were employed to scale the data by using a four-point smoothing curve. The data were corrected for Lorentz and polarization effects, and an analytical absorption correction was applied.[22] Pertinent crystallographic and experimental parameters for complexes **1a**, **2**, **3**, and **4**, are summarized in Table III.

The structures of **1a**, **2**, **3**, and **4**, were solved by conventional heavy-atom methods and were refined by full-matrix least-squares techniques, minimizing the function $\sum w(|F_o| - |F_c|)^2$, where w was calculated from $w = [(\sigma(F_o))^2 + 0.0003F_o^2]^{-1}$. During the refinement of **1a**, the reflection 023 showed extinction effects, and so it was omitted. All hydrogen atoms were located in difference Fourier maps and were included in the refinement with fixed isotropic temperature factors. The variables included in the refinement of **1a** were positional and anisotropic thermal parameters for all the non-hydrogen atoms and positional parameters for the hydrogen atoms. All the hydrogen atoms were located in difference Fourier maps of **2** and were included in the refinement with fixed isotropic temperatures factors. The variables included in the refinement of **2** were a scale factor, positional parameters for all atoms, and anisotropic thermal parameters for all the non-hydrogen atoms.

During the refinement of **3**, one of the benzyl groups exhibited disorder and was modeled with two isotropic sites for each meta, ortho, and para carbon atom. A single occupancy parameter was refined for these sites such that the net occupancy for each carbon atom was 1 [C(13)–C(17) occupancy = 0.60 (3); C(113)–C(117) occupancy = 0.40 (3); see Table IV]. Restraints on the bond distances and interbond angles in this ring were applied to the coordinate shifts during the refinement. Anisotropic temperature factors were refined for all unsplit non-hydrogen sites. A common isotropic temperature factor was refined for the hydrogen atoms. The refinement was considered complete when the maximum ratio of calculated shift to esd was less than 0.1. During the final cycles of the refinement, the weighting scheme employed was $w = 1/[18.947t_0(x) + 26.378t_1(x) + 9.457t_2(x)]$ where $x = |F_o|/F_{max}$ and t_n (n = 0, 1, 2) are the polynomial functions of the Chebyshev series. The largest peak in the final difference map was of height 0.9 (2) e Å^{-3} situated 0.90 Å from the tungsten atom.

The tungsten complex **4** is approximately isomorphous with its molybdenum analogue **2**, and the position of the molybdenum atom was used for the tungsten coordinates. The remaining non-hydrogen atoms were located in Fourier maps. The majority of the hydrogen atoms were located in the difference Fourier maps; those not located were placed geometrically. The variables included in the refinement of **4** were a scale factor and positional parameters and anisotropic temperature factors for the non-hydrogen atoms. Six reflections that possessed asymmetric backgrounds were omitted from the refinement.

The final residuals R, R_w, goodness of fit (GOF), and highest residual density for all the refinements of complexes **1a**, **2**, **3**, and **4** are listed in Table III. The refinements were considered complete when the ratios of all shifts to esd's were less than 0.1. Complex neutral-atom scattering factors were taken from ref 23. The computations were performed on a MICROVAX II computer using the NRC VAX crystal structure package[24] and the CRYSTALS suite of programs.[25] Final positional and equivalent isotropic thermal parameters ($U_{eq} = \frac{1}{3} \times$ trace of diagonalized U) for the complexes **1a**, **2**, **3**, and **4** are given in Table IV. Bond lengths (Å) and bond angles (deg) for all the bis(benzyl) nitrosyl complexes are listed in Tables V and VI, respectively. Anisotropic thermal parameters, the remaining molecular dimensions (including hydrogen atom coordinates), and tables of calculated and observed structure factors for all the complexes are provided as supplementary material. Views of the solid-state molecular structures of $CpMo(NO)(CH_2Ph)_2$ (**1a**), $Cp^*Mo(NO)(CH_2Ph)_2$ (**2**), $CpW(NO)(CH_2Ph)_2$ (**3**), and $Cp^*W(NO)(CH_2Ph)_2$ (**4**) are presented in Figures 7, 9, 10, and 11, respectively.[26]

X-ray Crystallographic Analysis of $CpMo(NO)(CH_2C_6H_2\text{-}2,4,6\text{-}Me_3)_2$ (1b). Large red crystals of **1b** were prepared by slow crystallization of the complex from CH_2Cl_2/hexanes at room temperature. A single crystal of the compound was

---

[21] Nugent, W. A.; Mayer, J. M. *Metal-Ligand Multiple Bonds*; Wiley Interscience: New York, 1988; Chapter 4.

[22] Alcock, N. W. In *Crystallographic Computing*; Ahmed, F. R., Ed.; Munksgaard: Copenhagen, 1969; p 271.

[23] *International Tables for X-ray Crystallography*; Kynoch Press: Birmingham, England, 1974; Vol. IV, Tables 2.2B and 2.3.1.

[24] Larson, A. C.; Lee, F. L.; Le Page, Y.; Gabe, E. J. *The NRC VAX Crystal Structure System*; Chemistry Division, National Research Council: Ottawa, Canada, 1984.

[25] Watkin, D. J.; Carruthers, J. R.; Betteridge, P. W. *CRYSTALS User Guide*; Chemical Crystallography Laboratory, University of Oxford; Oxford, U.K., 1985.

[26] Davies, E. K. *SNOOPI Plot Program*; Chemical Crystallography Laboratory, University of Oxford; Oxford, U.K., 1984.

Table II. Variable-Temperature ^{1}H and ^{13}C{^{1}H} NMR Data for the Bis(benzyl) Nitrosyl Complexes[a]

NMR data ($\mathrm{CD_2Cl_2}$), δ	
^{1}H	^{13}C{^{1}H}[b]
$\mathrm{CpMo(NO)(CH_2Ph)_2}$	
300 K	
7.32 (m, 6 H, $\mathrm{CH_2C_6}H_5$) 6.80 (m, 4 H, $\mathrm{CH_2C_6}H_5$) 5.37 (s, 5 H, $\mathrm{C_5}H_5$) 2.40 (d, 2 H, $\mathrm{C}H_a\mathrm{H_b}$, ${}^2J_{\mathrm{H_aH_b}} = 6.6$ Hz) 1.22 (d, 2 H $\mathrm{CH_a}H_b$, ${}^2J_{\mathrm{H_aH_b}} = 6.6$ Hz)	130.2, 129. 127.9 (aromatic Ph *C*) 101.3 ($C_5\mathrm{H_5}$) 35.91 ($C\mathrm{H_2}$)
183 K	
7.85–6.10 (m, 10 H, $\mathrm{CH_2C_6}H_5$) 5.36 (s, 5 H, $\mathrm{C_5}H_5$) 3.19 (d, 1 H, η^2-$\mathrm{C}H_a\mathrm{H_bC_6H_5}$, ${}^2J_{\mathrm{H_aH_b}} = 4.2$ Hz) 2.67 (d, 1 H, η^2-$\mathrm{CH_a}H_b\mathrm{C_6H_5}$, ${}^2J_{\mathrm{H_aH_b}} = 4.2$ Hz) 1.62 (d, 1 H, η^1-$\mathrm{C}H_a\mathrm{H_xC_6H_5}$, ${}^2J_{\mathrm{H_aH_x}} = 8.7$ Hz) −1.08 (d, 1 H, η^1-$\mathrm{CH_a}H_x\mathrm{C_6H_5}$, ${}^2J_{\mathrm{H_aH_x}} = 8.7$ Hz)	152.7 (quaternary η^1-$\mathrm{CH_2}C_6\mathrm{H_5}$) 139.6, 132.9, 129.6, 127.5, 126.2, 123.5, 121.5 (aromatic Ph *C*) 111.2 (quaternary η^2-$\mathrm{CH_2}C_6\mathrm{H_5}$) 100.4 ($C_5\mathrm{H_5}$) 36.8 ($\eta^1$-$C\mathrm{H_2C_6H_5}$) 32.3 ($\eta^2$-$C\mathrm{H_2C_6H_5}$)
$\mathrm{CpMo(NO)(CH_2C_6H_2\text{-}2,4,6\text{-}Me_3)_2}$	
300 K	
6.25 (m, 4 H, $\mathrm{CH_2C_6}H_2$) 4.62 (s, 5 H, $\mathrm{C_5}H_5$) 2.30 (br s, 4 H, $\mathrm{C}H_2\mathrm{C_6H_2}$) 1.82 (s, 12 H, $\mathrm{CH_2C_6H_2(C}H_3)_3$) 1.56 (s, 6 H, $\mathrm{CH_2C_6H_2(C}H_3)_3$)	129.7 (aromatic Ph *C*) 101.9 ($C_5\mathrm{H_5}$) 32.7 ($C\mathrm{H_2C_6H_2}$) 21.4 ($\mathrm{C_6H_2(}C\mathrm{H_3)_3}$) 20.8 ($\mathrm{C_6H_2(}C\mathrm{H_3)_3}$)
208 K	
6.29–6.15 (m, 4 H, $\mathrm{CH_2C_6}H_2$) 4.58 (s, 5 H, $\mathrm{C_5}H_5$) 2.83 (d, 1 H, η^1-$\mathrm{C}H_a\mathrm{H_bC_6H_2}$, ${}^2J_{\mathrm{H_aH_b}} = 5.7$ Hz) 2.71 (d, 1 H, η^1-$\mathrm{CH_a}H_b\mathrm{C_6H_2}$, ${}^2J_{\mathrm{H_aH_b}} = 5.7$ Hz) 1.64 (d, 1 H, η^2-$\mathrm{C}H_a\mathrm{H_xC_6H_2}$, ${}^2J_{\mathrm{H_aH_x}} = 8.3$ Hz) 1.89, 1.67, 1.60, 1.55, 1.47, 1.27 (s, 6 × (3 H), $\mathrm{CH_2C_6H_2(C}H_3)_3$) −2.45 (d, 1 H, η^2-$\mathrm{CH_a}H_x\mathrm{C_6H_2}$, ${}^2J_{\mathrm{H_aH_x}} = 8.3$ Hz)	149.2, 148.9, 144.9, 143.6 (quaternary η^1-$\mathrm{CH_2}C_6\mathrm{H_2(CH_3)_3}$) 132.9, 132.1, 130.1, 130.0, 127.8, 127.5 (aromatic Ph *C*) 104.3 (quaternary η^2-$\mathrm{CH_2}C_6\mathrm{H_2}$) 101.3 ($C_5\mathrm{H_5}$) 32.8 ($\eta^1$-$C\mathrm{H_2C_6H_2}$) 30.2 ($\eta^2$-$C\mathrm{H_2C_6H_2}$) 21.6, 21.0, 20.8, 20.3, 20.0, 19.5 ($\mathrm{CH_2C_6H_2(}C\mathrm{H_3)_3}$)
$\mathrm{Cp^*Mo(NO)(CH_2Ph)_2}$	
300 K	
7.16 (m, 6 H, $\mathrm{CH_2C_6}H_5$) 6.68 (d, 4 H, $\mathrm{CH_2C_6}H_5$) 2.31 (d, 2 H, $\mathrm{C}H_a\mathrm{H_b}$, ${}^2J_{\mathrm{H_aH_b}} = 7.5$ Hz) 1.77 (s, 15 H, $\mathrm{C_5(C}H_3)_5$) 0.36 (d, 2 H, $\mathrm{CH_a}H_b$, ${}^2J_{\mathrm{H_aH_b}} = 7.5$ Hz)	131.0, 128.0, 126.7 (aromatic Ph *C*) 108.97 ($C_5\mathrm{(CH_3)_5}$) 44.12 ($C\mathrm{H_2}$) 10.37 ($\mathrm{C_5(}C\mathrm{H_3)_5}$)
183 K	
7.75 (t, 10 H, $\mathrm{CH_2C_6}H_5$) 7.6–6.6 (m, 10 H, $\mathrm{CH_2C_6}H_5$) 5.53 (d, 10 H, $\mathrm{CH_2C_6}H_5$) 3.31 (d, 1 H, η^2-$\mathrm{C}H_a\mathrm{H_bC_6H_5}$, ${}^2J_{\mathrm{H_aH_b}} = 6.6$ Hz) 1.81 (d, 1 H, η^2-$\mathrm{CH_a}H_b\mathrm{C_6H_5}$, ${}^2J_{\mathrm{H_aH_b}} = 6.6$ Hz) 1.68 (s, 15 H, $\mathrm{C_5(C}H_3)_5$) 1.16 (d, 1 H, η^1-$\mathrm{C}H_a\mathrm{H_xC_6H_5}$, ${}^2J_{\mathrm{H_aH_x}} = 9.3$ Hz) −1.75 (d, 1 H, η^1-$\mathrm{C_a}H_x\mathrm{C_6H_5}$, ${}^2J_{\mathrm{H_aH_x}} = 9.3$ Hz)	152.8 (quaternary η^1-$\mathrm{CH_2}C_6\mathrm{H_5}$) 139.4, 131.6, 139.3, 127.6, 126.9, 121.3, (aromatic Ph *C*) 115.0 (quaternary η^2-$\mathrm{CH_2}C_6\mathrm{H_5}$) 108.4 ($C_5\mathrm{(CH_3)_5}$) 44.2 ($\eta^1$-$C\mathrm{H_2C_6H_5}$) 40.3 ($\eta^2$-$C\mathrm{H_2C_6H_5}$) 9.5 ($\mathrm{C_5(CH_3)_5}$)
$\mathrm{CpW(NO)(CH_2Ph)_2}$	
300 K	
7.26 (m, 6 H, $\mathrm{CH_2C_6}H_5$) 6.75 (m, 4 H, $\mathrm{CH_2C_6}H_5$) 5.33 (s, 5 H, $\mathrm{C_5}H_5$) 2.15 (d, 2 H, $\mathrm{C}H_a\mathrm{H_b}$, ${}^2J_{\mathrm{H_aH_b}} = 7.8$ Hz) 1.15 (d, 2 H, $\mathrm{CH_a}H_b$, ${}^2J_{\mathrm{H_aH_b}} = 7.9$ Hz)	130.4, 128.6, 127.7 (aromatic Ph *C*) 100.0 ($C_5\mathrm{H_5}$) 33.0 ($C\mathrm{H_2}$, ${}^1J_{\mathrm{CW}} = 59.0$ Hz)
183 K	
8.0 (t, 10 H, $\mathrm{CH_2C_6}H_5$) 7.6–6.6 (m, 10 H, $\mathrm{CH_2C_6}H_5$) 6.25 (d, 10 H, $\mathrm{CH_2C_6}H_5$) 5.46 (s, 5 H, $\mathrm{C_5}H_5$) 3.13 (d, 1 H, η^2-$\mathrm{C}H_a\mathrm{H_bC_6H_5}$, ${}^2J_{\mathrm{H_aH_b}} = 5.3$ Hz) 2.64 (d, 1 H, η^2-$\mathrm{CH_a}H_b\mathrm{C_6H_5}$, ${}^2J_{\mathrm{H_aH_b}} = 5.4$ Hz) 1.37 (d, 1 H, η^1-$\mathrm{C}H_a\mathrm{H_xC_6H_5}$, ${}^2J_{\mathrm{H_aH_x}} = 10.0$ Hz) −0.72 (d, 1 H, η^1-$\mathrm{CH_a}H_x\mathrm{C_6H_5}$, ${}^2J_{\mathrm{H_aH_x}} = 10.0$ Hz)	152.3 (quaternary η^1-$\mathrm{CH_2}C_6\mathrm{H_5}$) 140.5, 133.5, 130.3, 128.1, 127.4, 126.7, 126.0, 121.8, (aromatic Ph *C*) 108.6 (quaternary η^2-$\mathrm{CH_2}C_6\mathrm{H_5}$) 99.6 ($C_5\mathrm{H_5}$) 35.1 ($\eta^1$-$C\mathrm{H_2C_6H_5}$) 35.0 ($\eta^2$-$C\mathrm{H_2C_6H_5}$)

Table II (Continued)

NMR data (CD_2Cl_2), δ	
^1H	$^{13}C\{^1H\}^b$
$Cp^*W(NO)(CH_2C_6H_5)_2$[c]	
300 K	
7.16 (m, 6 H, $CH_2C_6H_5$) 6.82 (d, 4 H, $CH_2C_6H_5$) 2.24 (d, 2 H, CH_aH_b, $^2J_{H_aH_b}$ = 9.11 Hz) 1.81 (s, 15 H, $C_5(CH_3)_5$) 0.55 (d, 2 H, CH_aH_b, $^2J_{H_aH_b}$ = 9.11 Hz)	133.6, 132.1, 128.4, 127.1 (aromatic Ph C) 108.2 ($C_5(CH_3)_5$) 42.9 (CH_2) 10.3 ($C_5(CH_3)_5$)

[a] Cp = η^5-C_5H_5 and Cp* = η^5-C_5Me_5. [b] All signals are singlets unless indicated otherwise. [c] Cooling the CD_2Cl_2 solution of this compound to 183 K did not achieve a limiting spectrum; indeed, coalescence was maintained down to this temperature.

Table III. Crystallographic and Experimental Data[a] for the Complexes Cp′M(NO)(CH_2Ph')$_2$ (Cp′ = Cp or Cp*; M = Mo or W; Ph′ = C_6H_5 or $C_6H_2Me_3$) (1a, 1b, 2, 3, 4)

	1a	1b	2	3	4
formula	$C_{19}H_{19}NOMo$	$C_{25}H_{31}NOMo$	$C_{24}H_{29}NOMo$	$C_{19}H_{19}NOW$	$C_{24}H_{29}NOW$
fw	373.31	457.47	445.43	461.22	531.35
cryst syst	orthorhombic	triclinic	monoclinic	orthorhombic	monoclinic
space group	*Pbca*	$P\bar{1}$	$P2_1/c$	*Pbca*	$P2_1/c$
a, Å	10.122 (1)	9.4113 (19)	13.969 (5)	10.110 (1)	13.916 (4)
b, Å	15.625 (2)	8.3499 (18)	16.125 (3)	15.614 (2)	16.101 (3)
c, Å	20.770 (2)	15.4533 (18)	9.778 (5)	20.654 (2)	9.757 (3)
α, deg		98.004 (18)			
β, deg		100.408 (15)	110.67 (4)		110.08 (2)
γ, deg		110.511 (6)			
V, Å^3	3284.9	1091.3 (4)	2060.7	3260.4	2053.3
Z	8	2	4	8	4
d_{calcd}, Mg/m^{-3}	1.51	1.39	1.43	2.12	1.72
F(000)	1520	476	920	1776	1048
μ(Mo Kα), mm^{-1}	0.780	0.6024	0.633	7.251	5.758
T, K	293	295	208	293	211
cryst dimens, mm^3	0.36 × 0.38 × 0.21	0.23 × 0.24 × 0.34	0.15 × 0.15 × 0.32	0.34 × 0.37 × 0.32	0.34 × 0.20 × 0.38
λ(Mo Kα), Å	0.71069	0.71069	0.71069	0.71069	0.71069
transm factors	0.76–0.84[b]	0.86–0.89	0.88–0.93[b]	0.17–0.23[b]	0.17–0.36[b]
scan type	coupled ω–2θ	coupled ω–2θ	coupled ω–2θ	coupled ω–2θ	coupled ω–2θ
scan range, deg	0.65 + 0.35 tan θ	1.00 + 0.35 tan θ	0.70 + 0.35 tan θ	0.70 + 0.35 tan θ	0.85 + 0.35 tan θ
scan speed, deg/min	0.59–2.75	1.83–2.01	0.66–2.75	0.61–2.75	0.72–2.75
2θ limits, deg	$2 \le 2\theta \le 52$	$0 \le 2\theta \le 55$	$2 \le 2\theta \le 52$	$2 \le 2\theta \le 54$	$2 \le 2\theta \le 53$
data collected	*h*,*k*,*l*	±*h*,±*k*,*l*	*h*,*k*,±*l*	*h*,*k*,*l*	±*h*,*k*,*l*
no. of unique reflns	3225	4959	4068	3251	4248
no. of reflns with $I > 3\sigma(I)$	2057	3983	2775	2192	3471
no. of variables	256	377	331	192	244
R_F[c]	0.024	0.031	0.029	0.025	0.021
R_{wF}[d]	0.031[e]	0.039[f]	0.038[e]	0.028[e]	0.030[e]
goodness of fit[g]	1.218	1.249	1.179	1.286	1.212
max Δ/σ (final cycle)	0.1	0.03	0.1	0.1	0.1
residual density, e/Å^3	0.29 (5)	0.81	0.52 (7)	0.9 (2)	0.80 (11)

[a] Enraf-Nonius CAD4-F diffractometer, Mo Kα radiation, graphite monochromator. [b] Transmission coefficients were calculated by using a ϕ-scan-checked analytical correction. [c] $R_F = \sum||F_o| - |F_c||/\sum|F_o|$. [d] $R_{wF} = [\sum w(|F_o| - |F_c|)^2/\sum F_o^2]^{1/2}$. [e] $w = [(\sigma(F))^2 + 0.0003F^2]^{-1}$. [f] $w = [\sigma^2(F)]^{-1}$. [g] GOF = $[\sum w(|F_o| - |F_c|)^2/(\text{no. of degrees of freedom})]^{1/2}$.

mounted in a thin-walled capillary under N_2 and transferred to an Enraf-Nonius CAD4-F diffractometer. Data collection was carried out with graphite-monochromated Mo Kα radiation ($\lambda_{K\alpha_1}$ = 0.709 30, $\lambda_{K\alpha_2}$ = 0.713 59 Å). Three standard reflections, measured every hour of X-ray exposure time, showed no significant variations in intensity (ca. 0.5% isotropic). Least-squares analysis of 2(sin θ)/λ values for 25 well-centered, high-angle reflections gave the final unit cell parameters. The data were corrected for Lorentz and polarization effects and for absorption by using the Gaussian integration method.[27-29] The pertinent crystallographic and experimental data for **1b** are summarized in Table III.

The structure was determined by Patterson and electron density methods and refined by full-matrix least-squares methods on *F*, minimizing the function $\sum w(|F_o| - |F_c|)^2$, where *w* was calculated from $w = [\sigma^2(F)]^{-1}$. Hydrogen atoms, located in the difference Fourier maps, were included in the refinement. Refined variables were a scale factor, positional and anisotropic thermal parameters for non-hydrogen atoms, and positional and isotropic thermal parameters for hydrogen atoms. Final convergence was reached at *R* = 0.031; the maximum parameter shift during the last cycle of refinement was 0.033σ. Complex neutral-atom scattering factors were taken from ref 23. Final positional and equivalent isotropic thermal parameters (U_{eq} = $^1/_3$ × trace of diagonalized *U*) for complex **1b** are given in Table IV. Selected bond lengths (Å) and bond angles (deg) for the compound are listed in Tables V and VI, respectively. Anisotropic thermal parameters, the remaining molecular dimensions (including hydrogen atom coordinates), and tables of calculated and observed structure factors for **1b** are provided as supplementary material. A view of the solid-state molecular structure of CpMo(NO)($CH_2C_6H_2$-2,4,6-Me_3)$_2$ (**1b**) is displayed in Figure 8.

Results and Discussion

Syntheses of the Complexes Cp′M(NO)(CH_2Ph')$_2$ (Cp′ = Cp or Cp*; M = Mo or W; Ph′ = C_6H_5 or C_6H_2-2,4,6-Me_3). The methodology for the preparation of these bis(benzyl) complexes is similar to that described by us previously for the synthesis of the related series of

---

[27] The computer programs used include locally written programs for data processing and locally modified versions of the following: ORFLS, full-matrix least squares, and ORFFE, function and errors, by W. R. Busing, K. O. Martin, and H. A. Levy; FORDAP, Patterson and Fourier syntheses, by A. Zalkin; ORTEPII, illustrations, by C. K. Johnson.

[28] Coppens, P.; Leiserowitz, L.; Rabinovich, D. *Acta Crystallogr.* **1965**, *18*, 1035.

[29] Busing, W. R.; Levy, H. A. *Acta Crystallogr.* **1967**, *22*, 457.

Table IV. Final Positional (Fractional, ×10^4; Mo and W, ×10^6) and Isotropic Thermal Parameters (U_{eq} × 10^3, Å^2) for the Non-Hydrogen Atoms of the Complexes Cp′M(NO)(CH$_2$Ph)$_2$ (Cp′ = Cp or Cp*; Mo or W) (1a, 2, 3, 4) and CpMo(NO)(CH$_2$C$_6$H$_2$-2,4,6-Me$_3$)$_2$ (1b)

atom	x	y	z	U_{eq}	atom	x	y	z	U_{eq}
CpMo(NO)(CH$_2$Ph)$_2$									
Mo	173418 (24)	96330 (17)	93756 (12)	43.9	N	2377 (3)	−21 (2)	676 (1)	50
O	2702 (3)	−720 (2)	494 (1)	81.2	C(1)	−151 (4)	−557 (3)	1478 (2)	75.9
C(2)	−444 (4)	567 (4)	820 (2)	82.3	C(3)	−399 (4)	1393 (4)	616 (3)	92.7
C(4)	−101 (5)	1913 (3)	1129 (3)	100	C(5)	51 (4)	1385 (4)	1668 (2)	85.6
C(11)	2296 (4)	1581 (3)	25 (2)	75	C(12)	3460 (4)	1778 (2)	399 (2)	60.9
C(13)	4656 (4)	1317 (2)	364 (2)	61.9	C(14)	5685 (4)	1488 (3)	758 (2)	73.4
C(15)	5583 (5)	2118 (3)	1212 (2)	86.9	C(16)	4452 (7)	2580 (3)	1280 (2)	91.6
C(17)	3395 (5)	2401 (2)	882 (2)	75	C(21)	2918 (3)	892 (2)	1853 (2)	45
C(22)	2616 (3)	146 (2)	2261 (1)	44.6	C(23)	1877 (3)	227 (3)	2817 (2)	63.8
C(24)	1621 (4)	−468 (4)	3208 (2)	87.3	C(25)	2087 (5)	−1248 (4)	3063 (3)	94.3
C(26)	2812 (5)	−1358 (3)	2512 (3)	87.4	C(27)	3086 (4)	−661 (3)	2114 (2)	63.1
CpMo(NO)(CH$_2$C$_6$H$_2$-2,4,6-Me$_3$)$_2$									
Mo	55120 (20)	129520 (30)	832620 (10)	33	N	512 (3)	−851 (3)	8231 (2)	42
O	207 (3)	−2382 (3)	8228 (2)	67	C(1)	−2094 (4)	620 (7)	7825 (3)	67
C(2)	−1844 (4)	221 (6)	8651 (3)	64	C(3)	−1017 (5)	1754 (7)	9289 (3)	75
C(4)	−772 (5)	3144 (6)	8837 (4)	81	C(5)	−1450 (5)	2402 (7)	7931 (3)	76
C(11)	2455 (4)	2342 (4)	9562 (2)	48	C(12)	3395 (3)	3042 (3)	8952 (2)	40
C(13)	3631 (3)	4753 (3)	8793 (2)	46	C(14)	4433 (4)	5329 (4)	8156 (2)	52
C(15)	5014 (3)	4327 (4)	7657 (2)	55	C(16)	4839 (3)	2690 (4)	7835 (2)	51
C(17)	4063 (3)	2036 (4)	8469 (2)	43	C(18)	3141 (5)	6020 (5)	9330 (3)	61
C(19)	5884 (6)	4979 (9)	6968 (5)	87	C(20)	4083 (5)	324 (5)	8662 (3)	57
C(21)	936 (3)	1515 (4)	6939 (2)	37	C(22)	−320 (3)	1518 (3)	6204 (2)	34
C(23)	−1449 (3)	−60 (3)	5641 (2)	40	C(24)	−2608 (3)	−7 (4)	4963 (2)	48
C(25)	−2718 (3)	1547 (5)	4820 (2)	50	C(26)	−1603 (4)	3080 (4)	5364 (2)	46
C(27)	−403 (3)	3112 (3)	6045 (2)	39	C(28)	−1401 (5)	−1794 (4)	5760 (3)	54
C(29)	−4014 (5)	1554 (8)	4079 (3)	76	C(30)	826 (5)	4851 (4)	6586 (2)	58
Cp*Mo(NO)(CH$_2$Ph)$_2$									
Mo	702516 (23)	943854 (18)	898460 (30)	22.6	N	6008 (2)	10165 (2)	8388 (3)	48.4
O	5261 (2)	10585 (2)	7793 (4)	46	C(1)	7154 (3)	9065 (2)	6763 (4)	24
C(2)	6274 (3)	8661 (2)	6889 (4)	27.5	C(3)	6624 (3)	8068 (2)	8025 (4)	28.6
C(4)	7706 (3)	8094 (2)	8606 (4)	26.8	C(5)	8045 (3)	8703 (2)	7825 (4)	24
C(6)	7140 (4)	9660 (3)	5585 (5)	34.4	C(7)	5189 (3)	8793 (3)	5919 (5)	39.5
C(8)	5949 (4)	7440 (3)	8387 (5)	44.3	C(9)	8377 (4)	7522 (3)	9771 (5)	38
C(10)	9117 (3)	8868 (3)	7960 (5)	33.9	C(11)	6470 (4)	8891 (3)	10616 (4)	34.7
C(12)	7162 (3)	9488 (2)	11595 (4)	33.6	C(13)	6818 (4)	10268 (3)	11897 (5)	38
C(14)	7506 (4)	10835 (3)	12750 (5)	45.1	C(15)	8542 (4)	10657 (3)	13296 (5)	46
C(16)	8898 (4)	9904 (3)	13011 (5)	44.2	C(17)	8210 (3)	9329 (3)	12142 (4)	38.7
C(21)	8217 (3)	10425 (2)	9448 (4)	28.5	C(22)	8228 (3)	11039 (2)	8304 (4)	27.1
C(23)	7385 (3)	11537 (2)	7566 (5)	34.7	C(24)	7415 (4)	12109 (3)	6515 (5)	40.3
C(25)	8287 (4)	12208 (3)	6181 (5)	43.9	C(26)	9123 (4)	11733 (3)	6898 (5)	41.9
C(27)	9094 (3)	11161 (2)	7938 (4)	32.9					
CpW(NO)(CH$_2$Ph)$_2$									
W	172040 (20)	95350 (10)	93350 (10)	38.8	N	2357 (5)	−32 (4)	669 (2)	45.0
O	2691 (6)	−737 (3)	482 (3)	71.9	C(1)	57 (8)	1397 (7)	1670 (4)	64.8
C(2)	−164 (7)	556 (6)	1482 (4)	60.6	C(3)	−468 (7)	568 (7)	816 (4)	70.0
C(4)	−416 (8)	1402 (8)	613 (4)	69.4	C(5)	−92 (9)	1918 (7)	1136 (5)	79.7
C(11)	2290 (8)	1587 (5)	36 (3)	62.2	C(12)	3462 (7)	1783 (4)	404 (3)	50.5
C(13)	4602 (13)	1283 (11)	331 (8)	50.7 (18)	C(14)	5690 (13)	1436 (10)	704 (8)	56.6 (22)
C(15)	5701 (14)	2043 (10)	1223 (6)	60.4 (24)	C(16)	4628 (17)	2545 (8)	1325 (6)	52.9 (22)
C(17)	3526 (15)	2427 (8)	916 (6)	50.5 (20)	C(113)	4726 (18)	1348 (16)	415 (12)	50.7 (18)
C(114)	5687 (18)	1562 (14)	829 (11)	56.6 (22)	C(115)	5388 (22)	2258 (14)	1218 (9)	60.4 (24)
C(116)	4166 (23)	2659 (11)	1211 (9)	52.9 (22)	C(117)	3120 (20)	2396 (11)	837 (9)	50.5 (20)
C(21)	2905 (5)	898 (4)	1839 (3)	40.7	C(22)	2617 (5)	144 (4)	2254 (3)	38.0
C(23)	1891 (6)	228 (5)	2822 (3)	57.2	C(24)	1621 (8)	−465 (7)	3214 (4)	65.6
C(25)	2090 (9)	−1247 (7)	3059 (5)	71.7	C(26)	2789 (9)	−1356 (5)	2504 (5)	69.9
C(27)	3083 (7)	−661 (4)	2106 (3)	50.8					
Cp*W(NO)(CH$_2$Ph)$_2$									
W	701061 (11)	943987 (9)	896062 (14)	21.8	N	6003 (3)	10157 (2)	8394 (4)	30.9
O	5240 (3)	10590 (2)	7785 (4)	45.8	C(1)	7146 (3)	9059 (2)	6750 (4)	25.2
C(2)	6263 (3)	8662 (2)	6865 (4)	27	C(3)	6608 (3)	8061 (2)	8005 (4)	27.5
C(4)	7700 (3)	8090 (2)	8603 (4)	25.8	C(5)	8040 (3)	8696 (2)	7812 (4)	24
C(6)	7149 (3)	9660 (3)	5562 (4)	33.6	C(7)	5177 (3)	8802 (3)	5905 (5)	37.1
C(8)	5941 (4)	7445 (3)	8392 (5)	44.3	C(9)	8353 (4)	7523 (3)	9743 (4)	36.8
C(10)	9115 (3)	8870 (3)	7946 (4)	33.3	C(11)	6486 (3)	8895 (3)	10617 (4)	33.2
C(12)	7191 (4)	9502 (3)	11608 (4)	34.3	C(13)	6836 (4)	10273 (3)	11913 (4)	36.7
C(14)	7501 (4)	10851 (3)	12757 (5)	42.3	C(15)	8544 (4)	10672 (3)	13316 (5)	44.7
C(16)	8910 (4)	9919 (3)	13039 (5)	40.5	C(17)	8233 (4)	9334 (3)	12174 (5)	38.1
C(21)	8220 (3)	10409 (2)	9453 (4)	26.7	C(22)	8225 (3)	11036 (2)	8311 (4)	26.8
C(23)	7364 (3)	11533 (3)	7573 (5)	33.8	C(24)	7403 (4)	12104 (3)	6536 (5)	38.1
C(25)	8284 (4)	12220 (3)	6200 (5)	44.1	C(26)	9140 (4)	11748 (3)	6925 (4)	41.8
C(27)	9103 (3)	11162 (3)	7955 (4)	30.8					

Table V. Selected Bond Lengths (Å) for the Complexes $Cp'M(NO)(CH_2Ph)_2$ (Cp' = Cp or Cp*; M = Mo or W) (1a, 2, 3, 4) and $CpMo(NO)(CH_2C_6H_2\text{-}2,4,6\text{-}Me_3)_2$ (1b)

	1a	1b[a]	2	3[b]	4
M–N	1.755 (2)	1.764 (2)	1.773 (3)	1.755 (5)	1.752 (3)
M–C(1)[c]	2.303 (4)	2.305 (4)	2.321 (4)	2.370 (7)	2.311 (3)
M–C(2)[c]	2.303 (4)	2.292 (4)	2.314 (4)	2.302 (7)	2.318 (4)
M–C(3)[c]	2.358 (4)	2.360 (5)	2.390 (3)	2.306 (8)	2.398 (4)
M–C(4)[c]	2.410 (4)	2.433 (5)	2.448 (3)	2.365 (7)	2.449 (4)
M–C(5)[c]	2.374 (4)	2.395 (5)	2.422 (3)	2.409 (8)	2.417 (4)
M–C(11)	2.203 (4)	2.196 (3)	2.191 (4)	2.179 (7)	2.173 (4)
M–C(12)	2.433 (3)	2.483 (3)	2.493 (4)	2.444 (6)	2.510 (4)
M–C(13)	3.236 (4)	3.172 (3)	3.250 (4)	3.209 (16)	3.261 (4)
M–C(17)	2.808 (5)	3.101 (3)	2.949 (5)	2.938 (14)	3.015 (4)
M–C(21)	2.251 (3)	2.259 (2)	2.231 (3)	2.223 (5)	2.223 (4)
N–O	1.203 (4)	1.207 (3)	1.208 (4)	1.215 (7)	1.239 (5)
C(1)–C(2)	1.399 (6)	1.364 (6)	1.435 (5)	1.388 (12)	1.423 (5)
C(1)–C(5)	1.366 (8)	1.369 (6)	1.433 (5)	1.379 (12)	1.441 (5)
C(1)–C(6)			1.495 (5)		1.512 (5)
C(2)–C(3)	1.361 (9)	1.375 (6)	1.416 (5)	1.409 (11)	1.427 (5)
C(2)–C(7)			1.492 (6)		1.497 (6)
C(3)–C(4)	1.374 (9)	1.409 (7)	1.415 (5)	1.369 (14)	1.429 (5)
C(3)–C(8)			1.508 (6)		1.493 (5)
C(4)–C(5)	1.399 (8)	1.382 (6)	1.423 (5)	1.386 (13)	1.423 (5)
C(4)–C(9)			1.508 (6)		1.483 (6)
C(5)–C(10)			1.481 (5)		1.482 (5)
C(11)–C(12)	1.445 (6)	1.452 (4)	1.457 (6)	1.441 (10)	1.483 (6)
C(12)–C(13)	1.411 (5)	1.422 (4)	1.413 (6)	1.400[d]	1.405 (6)
C(12)–C(17)	1.398 (6)	1.422 (4)	1.393 (6)	1.461[d]	1.389 (7)
C(13)–C(14)	1.351 (6)	1.384 (5)	1.375 (7)	1.364[d]	1.370 (7)
C(14)–C(15)	1.367 (7)	1.374 (5)	1.384 (7)	1.430[d]	1.394 (8)
C(15)–C(16)	1.361 (9)	1.391 (4)	1.377 (7)	1.356[d]	1.377 (7)
C(16)–C(17)	1.380 (9)	1.385 (7)	1.389 (7)	1.410[d]	1.394 (8)
C(21)–C(22)	1.472 (4)	1.486 (3)	1.497 (5)	1.486 (7)	1.505 (5)
C(22)–C(23)	1.383 (4)	1.409 (4)	1.397 (6)	1.389 (8)	1.414 (6)
C(22)–C(27)	1.382 (5)	1.412 (3)	1.393 (5)	1.377 (9)	1.396 (5)
C(23)–C(24)	1.381 (9)	1.386 (4)	1.392 (6)	1.379 (10)	1.381 (6)
C(24)–C(25)	1.340 (9)	1.382 (5)	1.377 (7)	1.348 (14)	1.387 (7)
C(25)–C(26)	1.371 (9)	1.373 (4)	1.365 (7)	1.357 (13)	1.384 (7)
C(26)–C(27)	1.394 (6)	1.389 (4)	1.385 (6)	1.394 (10)	1.392 (6)

[a] Average bond distances for PhC–CH_3 are 1.504 (7) and 1.508 (15) Å. [b] W–C(113) = 3.280 (24), W–C(117) = 2.668 (19), C(12)–C(113) = 1.447, C(12)–C(117) = 1.355, C(113)–C(114) = 1.337, C(114)–C(115) = 1.385, C(115)–C(116) = 1.385, C(116)–C(117) = 1.372 Å. [c] C(1)–C(5) constitute the cyclopentadienyl ring. [d] A restraint was applied to this bond.

thermally stable, 16-electron dialkyl nitrosyl complexes $Cp'M(NO)R_2$ (Cp' = Cp or Cp*; M = Mo or W; R = CH_2SiMe_3, CH_2CMe_3, or CH_2CMe_2Ph).[2,7] Thus, treatment of either the dichloro or diiodo nitrosyl precursors $Cp'M(NO)X_2$ (Cp' = Cp or Cp*; M = Mo or W; X = Cl or I) with 2 equiv of a benzyl Grignard reagent, $Ph'CH_2MgCl$ (Ph' = C_6H_5 or $C_6H_2\text{-}2,4,6\text{-}Me_3$), at 0 °C affords the corresponding bis(benzyl) nitrosyl complexes in good isolated yields (typically 50–65%), i.e.

$$Cp'M(NO)X_2 + 2\,Ph'CH_2MgCl \xrightarrow[2.\ H_2O,\ 25\ ^\circ C]{1.\ THF/Et_2O,\ 0\ ^\circ C} Cp'M(NO)(CH_2Ph')_2 + 2\,MgClX \quad (2)$$

As transformations 2 proceed, the reaction mixtures change from a brownish green to a dark red color, and a white to yellow precipitate forms. The addition of H_2O in the second step does not cause any color changes to occur but destroys any excess of the Grignard reagent present after the completion of the reaction and breaks up any $[Cp'M(NO)(CH_2Ph')_2]_2MgXCl$ adduct that might have been formed.[2,7] In order to simplify the workup, all the final reaction mixtures are first filtered through Celite to remove the insoluble MgClX product. The filtrates are then chromatographed on alumina to obtain solutions of the desired bis(benzyl) complexes, which are finally isolated as analytically pure crystalline materials by crystallization from hexanes/CH_2Cl_2 at −20 °C.

Physical and Spectroscopic Properties of the Bis(benzyl) Nitrosyl Complexes. All the bis(benzyl) nitrosyl complexes prepared in this work are relatively high melting (143–163 °C), orange-red, diamagnetic solids that are soluble in most common organic solvents such as benzene, toluene, Et_2O, and CH_2Cl_2. They are, for the most part, insoluble in hexanes or pentane, but the tungsten complexes do exhibit some solubility in these nonpolar solvents. As expected, the Cp* compounds exhibit greater solubilities than do their Cp analogues.

Unlike their dialkyl analogues $Cp'M(NO)R_2$ (M = Mo or W; R = CH_2SiMe_3, CH_2CMe_3, or CH_2CMe_2Ph), which are air-sensitive both in solutions and in the solid state,[8] these bis(benzyl) complexes, $Cp'M(NO)(CH_2Ph')_2$, exhibit only limited reactivity with dioxygen. Thus, they are all stable to air in the solid state for hours, and only solutions of the tungsten species react with O_2 to produce low yields (<20%) of the corresponding dioxo benzyl complexes, $Cp'W(O)_2(CH_2Ph')$. Solutions of the molybdenum species deposit a green precipitate when exposed to O_2 for several days at ambient temperatures, but no tractable organometallic complexes are isolable from the final mixtures.

The analytical and spectroscopic data for the new bis(benzyl) complexes 1a, 1b, 2, 3,[19] and 4 are summarized in Tables I and II. Signals due to the parent ion for each complex are observable in their 70-eV low-resolution mass spectra, a fact that is consistent with all the bis(benzyl) complexes being monomeric species. Their monomeric natures have been unequivocally established by single-crystal X-ray crystallographic analyses of all five complexes, which reveal that they possess pseudo four-legged piano-stool molecular structures in the solid state (vide infra).

The IR spectral features exhibited by these bis(benzyl) complexes merit some discussion in light of their molecular structures. All the bis(benzyl) compounds display single ν_{NO}'s in their IR spectra that fall within the range, i.e. 1640–1550 cm^{-1},[7,8] customarily associated with the existence of linear M–N–O linkages in $Cp'M(NO)R_2$ complexes.[30] The most chemically interesting feature of the IR spectrum of each $Cp'M(NO)(CH_2Ph')_2$ complex as a Nujol mull is that its ν_{NO} always occurs at a higher wavenumber than the ν_{NO} exhibited by its 16-electron dialkyl analogue, $Cp'M(NO)R_2$ (R = CH_2SiMe_3, CH_2CMe_3, and CH_2CMe_2Ph). For instance, the ν_{NO} observed at 1601 cm^{-1} in the Nujol mull IR spectrum of $CpMo(NO)(CH_2Ph)_2$ (1a) is higher in energy than the ν_{NO} at 1587 cm^{-1} exhibited by $CpMo(NO)(CH_2SiMe_3)_2$.[7] Furthermore, the ν_{NO} observed at 1570 cm^{-1} in the Nujol mull IR spectrum of $CpW(NO)(CH_2Ph)_2$ (3) is higher in wavenumber than the ν_{NO} exhibited by each of the complexes $CpW(NO)(CH_2SiMe_3)_2$, $CpW(NO)(CH_2CMe_3)_2$, and $CpW(NO)(CH_2CMe_2Ph)_2$, i.e. 1541, 1560, and 1540 cm^{-1}, respectively.[7] These observations indicate that there is less electron density available on the metal centers for π-back-bonding to the antibonding orbitals of the nitrosyl ligand in the 18-electron bis(benzyl) complexes than in their 16-electron dialkyl analogues. Such a situation would be expected if the bis(benzyl) complexes each contained two η^1-benzyl ligands, since an η^1-benzyl ligand is generally considered to be a poorer σ-donor than typical alkyl groups such as CH_2CMe_3 and CH_2CMe_2Ph. However, the bis(benzyl) complexes possess $Cp'M(NO)(\eta^1\text{-}CH_2Ph')(\eta^2\text{-}CH_2Ph')$ solid-state molecular structures and are formulated as 18-electron species by virtue of the interaction of the metal with the pπ-electron

---

(30) Shoulders on the ν_{NO} bands around 1595 cm^{-1}, due to phenyl H vibrations, are sometimes very intense and therefore make definitive assignments difficult.

Table VI. Selected Bond Angles (deg) for the Complexes $Cp'M(NO)(CH_2Ph)_2$ (Cp′ = Cp or Cp*; M = Mo or W) (1a, 2, 3, 4) and $CpMo(NO)(CH_2C_6H_2\text{-}2,4,6\text{-}Me_3)_2$ (1b)[a]

	1a	1b	2	3[b]	4
C(11)-M-N	91.3 (2)	93.28 (2)	93.3 (2)	92.1 (3)	93.7 (2)
C(12)-M-N	92.9 (1)	100.6 (1)	94.5 (1)	93.5 (2)	94.9 (1)
C(12)-M-C(11)	35.9 (2)	35.48 (10)	35.5 (1)	35.7 (3)	36.0 (2)
C(21)-M-N	91.2 (2)	94.80 (11)	92.9 (2)	91.7 (2)	94.0 (2)
C(21)-M-C(11)	127.7 (1)	123.4 (1)	124.8 (2)	126.2 (3)	123.0 (2)
C(21)-M-C(12)	91.8 (1)	88.04 (9)	89.3 (1)	90.5 (2)	87.1 (0)
M-N-O	174.1 (3)	166.5 (2)	170.0 (3)	174.7 (5)	169.7 (3)
C(5)-C(1)-C(2)	107.8 (4)	108.7 (4)	107.7 (3)	108.6 (8)	108.5 (3)
C(6)-C(1)-C(2)			125.4 (3)		125.3 (4)
C(6)-C(1)-C(5)			126.3 (3)		125.6 (3)
C(3)-C(2)-C(1)	108.0 (5)	108.6 (4)	107.7 (3)	107.1 (8)	107.3 (3)
C(7)-C(2)-C(1)			126.1 (4)		126.7 (4)
C(7)-C(2)-C(3)			126.0 (4)		125.9 (4)
C(4)-C(3)-C(2)	108.9 (5)	107.3 (4)	108.6 (3)	107.7 (9)	108.8 (3)
C(8)-C(3)-C(2)			124.4 (4)		125.1 (4)
C(8)-C(3)-C(4)			126.5 (4)		125.8 (4)
C(5)-C(4)-C(3)	107.3 (5)	106.9 (4)	108.4 (3)	108.9 (8)	107.8 (3)
C(9)-C(4)-C(3)			125.1 (4)		125.3 (4)
C(9)-C(4)-C(5)			126.3 (4)		126.6 (4)
C(4)-C(5)-C(1)	108.2 (4)	108.4 (4)	107.5 (3)	107.8 (9)	107.6 (3)
C(10)-C(5)-C(1)			125.7 (3)		125.6 (3)
C(10)-C(5)-C(4)			126.4 (4)		126.5 (4)
C(12)-C(11)-M	80.8 (2)	83.1 (2)	83.6 (2)	82.2 (4)	84.5 (2)
C(11)-C(12)-M	63.3 (2)	61.42 (15)	60.9 (2)	62.1 (4)	59.5 (2)
C(13)-C(12)-M	111.9 (2)	105.1 (2)	109.5 (3)	110.2 (9)	109.6 (3)
C(13)-C(12)-C(11)	124.3 (4)	120.7 (3)	121.9 (4)	120.1[c]	121.2 (4)
C(17)-C(12)-M	90.1 (2)	101.7 (2)	94.5 (2)	94.2 (6)	97.1 (3)
C(17)-C(12)-C(11)	119.8 (4)	121.5 (3)	119.6 (4)	124.4[c]	119.8 (4)
C(17)-C(12)-C(13)	115.6 (4)	117.8 (3)	118.1 (4)	115.2 (8)	118.8 (4)
C(14)-C(13)-C(12)	122.0 (4)	119.2 (3)	120.2 (4)	120.2[c]	120.9 (4)
C(15)-C(14)-C(13)	120.1 (4)	123.1 (3)	120.5 (4)	123.2[c]	119.5 (4)
C(16)-C(15)-C(14)	121.2 (5)	117.7 (3)	120.6 (4)	119.5[c]	120.7 (4)
C(17)-C(16)-C(15)	118.9 (4)	122.3 (3)	119.3 (4)	117.7[c]	119.7 (4)
C(16)-C(17)-C(12)	122.2 (4)	119.7 (3)	121.3 (4)	124.0[c]	120.4 (4)
C(22)-C(21)-M	114.4 (2)	121.0 (2)	121.5 (3)	114.2 (4)	120.4 (3)
C(23)-C(22)-C(21)	121.3 (3)	121.2 (2)	122.5 (4)	121.0 (6)	122.6 (3)
C(27)-C(22)-C(21)	121.7 (3)	120.6 (2)	121.6 (4)	121.7 (5)	120.6 (4)
C(27)-C(22)-C(23)	117.0 (3)	118.2 (2)	115.9 (4)	117.1 (6)	116.8 (4)
C(24)-C(23)-C(22)	121.4 (4)	119.6 (3)	121.5 (4)	121.7 (8)	120.7 (4)
C(25)-C(24)-C(23)	121.1 (4)	122.4 (3)	120.8 (4)	120.1 (7)	121.5 (4)
C(26)-C(25)-C(24)	119.4 (4)	117.6 (3)	118.8 (4)	119.9 (7)	118.7 (4)
C(27)-C(26)-C(25)	120.2 (5)	122.5 (3)	120.7 (4)	120.7 (8)	120.2 (4)
C(26)-C(27)-C(22)	121.0 (4)	119.5 (3)	122.4 (4)	120.5 (7)	122.0 (4)

[a] C(1)-C(5) constitute the cyclopentadienyl ring. [b] C(113)-C(12)-W = 112.3 (12), C(113)-C(12)-C(11) = 129.4, W-C(117)-C(12)-W = 83.9 (9), C(117)-C(12)-C(11) = 106.7, C(117)-C(12)-C(113) = 123.3 (11), C(114)-C(113)-C(12) = 122.2, C(115)-C(114)-C(113) = 114.2, C(116)-C(115)-C(114) = 122.9, C(117)-C(116)-C(115) = 124.0, C(116)-C(117)-C(12) = 112.6°. [c] A restraint was applied to this angle.

cloud of the η^2-benzyl ligand. If the extra electron density on the formally 18-electron metal center in each bis(benzyl) complex were available for back-bonding to the nitrosyl ligand, then a ν_{NO} lower than the ν_{NO} exhibited by its 16-electron dialkyl analogue would be expected. The IR spectral features displayed by the bis(benzyl) complexes indicate that this extra electron density is *not* available for M → NO backbonding, but it is not immediately apparent why this is so.

Variable-Temperature NMR Studies of the Bis(benzyl) Complexes 1a, 1b, 2, 3, and 4. The ^1H and $^{13}C\{^1H\}$ NMR spectral data for all the bis(benzyl) complexes are collected in Table II. At the outset, it may be noted that variable-temperature ^1H and $^{13}C\{^1H\}$ NMR spectroscopy of all the compounds in CD_2Cl_2 establishes that they are stereochemically nonrigid in solution and undergo the dynamic process

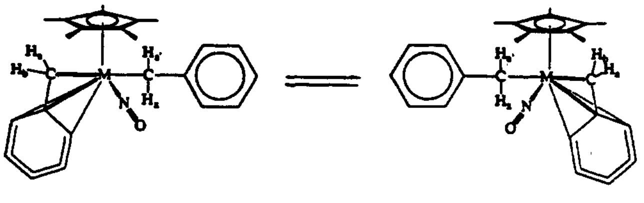

At room temperature, the rate of the fluxional process is fast on the NMR time scale, and so a time-averaged ^1H or $^{13}C\{^1H\}$ spectrum is obtained. In other words, at ambient temperatures, there are two magnetically equivalent sets of diastereotopic protons on the methylene carbon atoms of the benzyl ligands. At lower temperatures, the rate of the fluxional process is slower, and so two clearly different methylene carbon and phenyl group environments are evident in the ^1H and $^{13}C\{^1H\}$ NMR spectra. Representative ^1H and $^{13}C\{^1H\}$ NMR spectra of two bis(benzyl) complexes, namely those of $CpMo(NO)(CH_2C_6H_2\text{-}2,4,6\text{-}Me_3)_2$ (**1b**) and $Cp^*W(NO)(CH_2C_6H_5)_2$ (**4**), are presented in Figures 1 and 2, respectively, and the general features outlined above will now be considered in more specific detail.

The ambient-temperature ^1H NMR spectra of the bis(benzyl) complexes display, in addition to proton resonances due to either the Cp or Cp* ligand and the aromatic phenyl protons, a single AX pattern for the four methylene protons of the bis(benzyl) complex, the latter resonances being assigned by using the appropriate proton–proton decoupling experiments. One doublet of the AX pattern appears in the spectral region δ 2.4–2.0 ppm, while the other doublet appears upfield in the range δ 1.2–0.3 ppm,

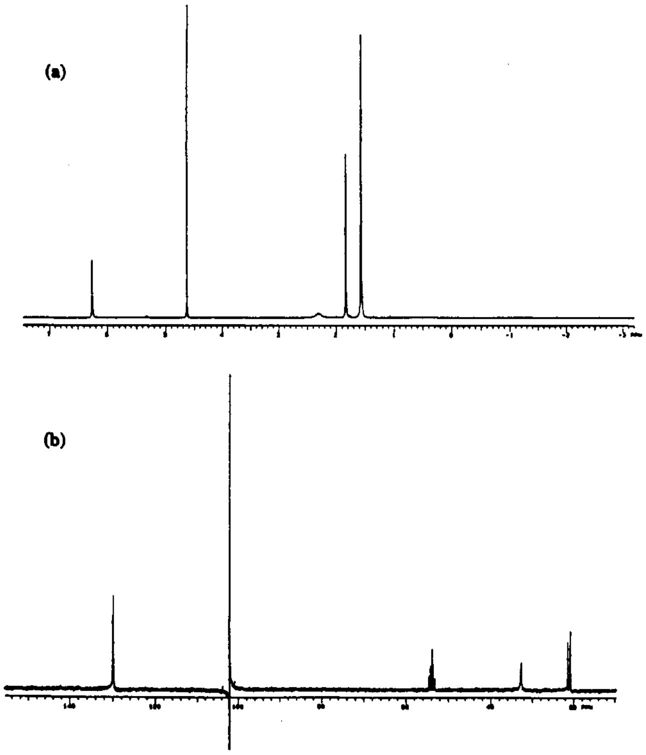

Figure 1. (a) 300-MHz ${}^1H$ and (b) 75-MHz ${}^{13}C\{{}^1H\}$ NMR spectra of $CpMo(NO)(CH_2C_6H_2\text{-}2,4,6\text{-}Me_3)_2$ (**1b**) in CD_2Cl_2 solution at ambient temperatures.

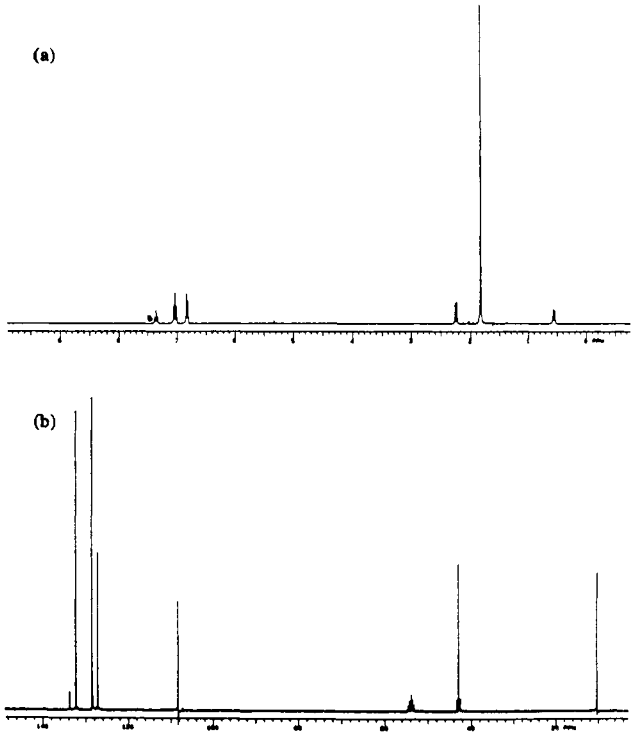

Figure 2. (a) 300-MHz ${}^1H$ and (b) 75-MHz ${}^{13}C\{{}^1H\}$ NMR spectra of $Cp^*W(NO)(CH_2Ph)_2$ (**4**) in CD_2Cl_2 solution at ambient temperatures.

and the ${}^2J_{H_aH_x}$ coupling constant varies between 6.6 and 9.1 Hz depending on the complex. As noted in the preceding paragraph, this AX pattern is diagnostic of two equivalent sets of diastereotopic methylene protons, i.e. $[Ph'CH_aH_x\text{–}M\text{–}CH_{a'}H_{x'}Ph']$, a feature consistent with the two benzyl groups being equivalent. These spectral features are clearly evident in the ${}^1H$ NMR spectrum of **4** shown in Figure 2a. Interestingly, the 300-MHz ${}^1H$ NMR spectrum of **1b** at ambient temperatures (Figure 1a) does not exhibit the expected AX pattern for the methylene protons due to coalescence of the signals. Furthermore, only two proton resonances are observed for the six methyl groups on the two benzyl ligands. These resonances may be attributed to the two equivalent para methyl and four equivalent ortho methyl substituents on the benzyl ligands, respectively.

The room-temperature ${}^{13}C\{{}^1H\}$ NMR spectrum of each bis(benzyl) complex generally exhibits only three or four carbon resonances for the twelve carbon atoms of the two benzyl groups (Table II). The exception of this generalization is complex **1b**, whose ${}^{13}C\{{}^1H\}$ NMR spectrum (Figure 1b) exhibits only one carbon resonance in the spectral region δ 160–115 ppm. Furthermore, each spectrum contains a single carbon resonance for the two methylene carbon atoms in the spectral region δ 44–33 ppm. Gated decoupled ${}^{13}C$ NMR spectra of **1a** and **1b** establish that the one-bond coupling constant between the two equivalent methylene carbon atoms and their two protons, i.e. ${}^1J_{CH}$, is 142.2 and 140.0 Hz, respectively.[31]

The features of the ${}^1H$ and ${}^{13}C\{{}^1H\}$ NMR spectra of each of the bis(benzyl) complexes are remarkably changed, however, upon cooling each complex in CD_2Cl_2 solution to approximately 183 K (see Table II). Compare, for instance, the 300-MHz ${}^1H$ and 75-MHz ${}^{13}C\{{}^1H\}$ NMR spectra of complex **1b** obtained at 208 K (Figure 3) with those obtained at room temperature (Figure 1). Striking changes are evident as the aromatic proton and carbon regions become much more complex, and all six methyl groups on the two benzyl ligands become inequivalent as the complex is cooled to lower temperatures.

At low temperatures, the ${}^1H$ NMR spectrum of each complex in CD_2Cl_2 solution exhibits, in addition to proton resonances due to either a Cp or Cp* ligand and the phenyl protons (Table II), four doublets that integrate for one proton each for the methylene protons of the two benzyl groups. Routine proton–proton decoupling experiments can be used to assign these doublets to a low-field AB pattern in the spectral region δ 3.31–1.81 ppm (with coupling of the two protons, ${}^2J_{H_aH_b}$, being between 4.2 and 6.6 Hz) and a high-field AX pattern in the spectral region δ +1.64 to −2.45 ppm (with coupling of the two protons, ${}^2J_{H_aH_x}$, being between 8.3 and 10.0 Hz). An illustration of these proton–proton decoupling experiments, using $CpMo(NO)(CH_2C_6H_5)_2$ (**1a**) as a representative example, is given in Figure 4. Similar decoupling experiments can be used to find the fourth doublet in the low-temperature ${}^1H$ NMR spectrum of **1b** shown in Figure 3a. Irradiation of the high-field doublet at −2.45 ppm causes a singlet to appear at ca. 1.64 ppm among the envelope of methyl resonances in the spectral region δ 1.89–1.47 ppm. The observed AB and AX patterns establish, therefore, that the two benzyl ligands of each bis(benzyl) complex are in very different environments in solution at low temperatures and that the two protons attached to each methylene carbon atom are diastereotopic. Unfortunately, the molecular structure of an individual bis(benzyl) complex in solution cannot be established unambiguously from its ${}^1H$ NMR data alone. For that, the pertinent ${}^{13}C$ NMR data are also required.

The low-temperature gated decoupled ${}^{13}C$ NMR spectra for complexes **1a**, **1b**, and **2** are also indicative of the two

---

[31] These values of ${}^1J_{CH}$ (i.e. 142.2 and 140.0 Hz) are exactly half the sum of the two values of ${}^1J_{CH}$ for the different methylene carbon resonances that are observed in the low-temperature gated decoupled ${}^{13}C$ NMR spectra of **1a** and **1b** (i.e.: for **1a**, ${}^1J_{CH}$ = 152.0 and 131.6 Hz; for **1b**, ${}^1J_{CH}$ = 150.1 and 130.7 Hz).

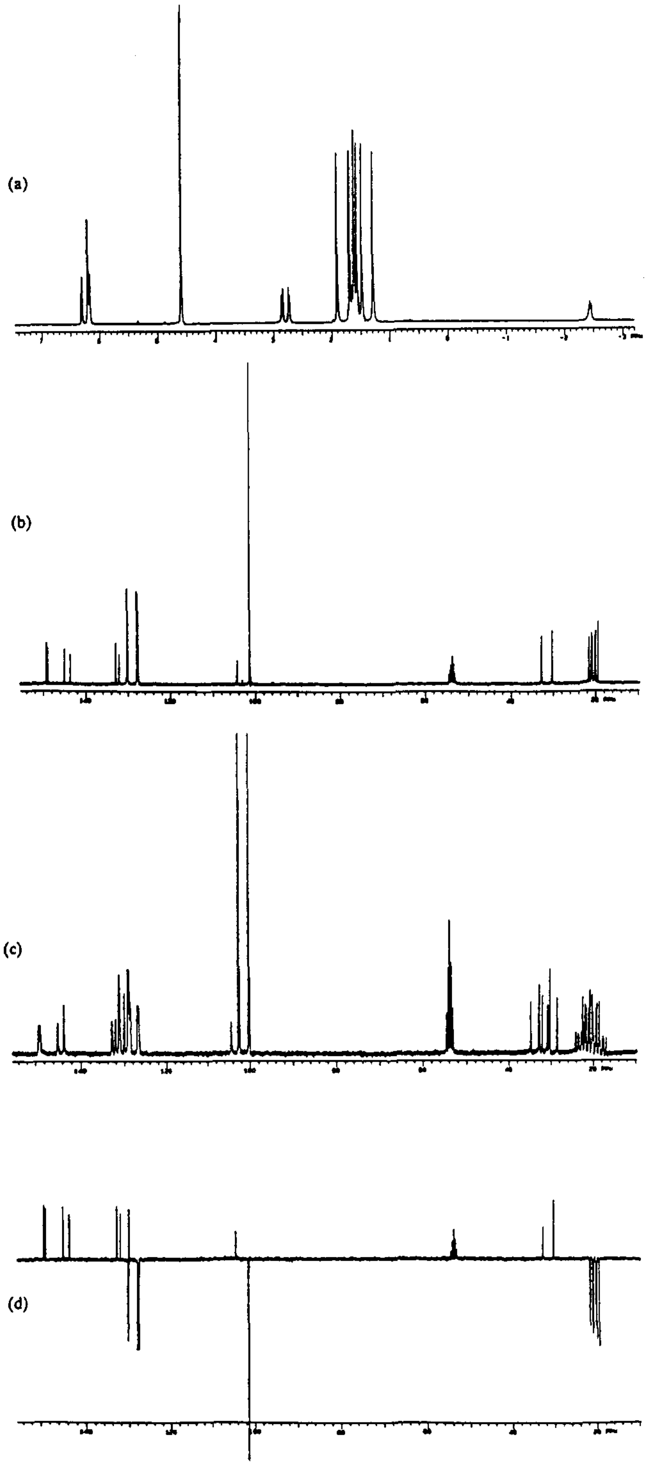

Figure 3. NMR spectra of $CpMo(NO)(CH_2C_6H_2\text{-}2,4,6\text{-}Me_3)_2$ (**1b**) in CD_2Cl_2 solution at 208 K: (a) 300-MHz ^1H NMR spectrum; (b) 75-MHz $^{13}C\{^1H\}$ NMR spectrum; (c) 75-MHz gated decoupled ^{13}C NMR spectrum; (d) 75-MHz (APT) ^{13}C NMR spectrum.

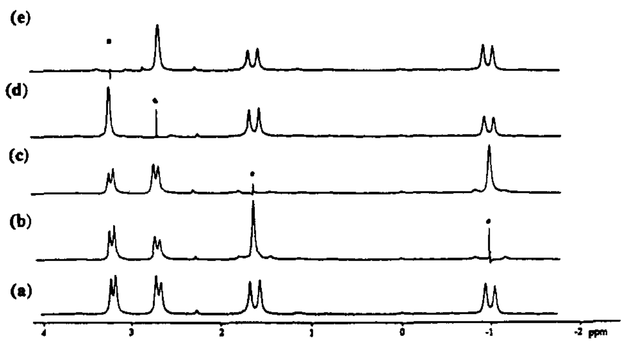

Figure 4. 80-MHz ^1H NMR spectra of $CpMo(NO)(CH_2Ph)_2$ (**1a**) in CD_2Cl_2 solution at 183 K. Proton–proton decoupling experiments: (a) methylene proton region of the undecoupled spectrum; (b) irradiation at −1.08 ppm; (c) irradiation at 1.62 ppm; (d) irradiation at 2.67 ppm; (e) irradiation at 3.19 ppm.

benzyl ligands being different at these temperatures. Not only are two carbon resonances observed for the methylene carbon atoms of the benzyl groups, but two very different carbon–proton coupling constants are also exhibited by the signals attributable to the different methylene carbon atoms. The low-field methylene carbon resonances in the ^{13}C NMR spectra of complexes **1a**, **1b**, and **2**, display $^1J_{CH}$ = 152.0, 150.1, and 148.2 Hz, respectively, while the high-field methylene carbon resonances exhibit $^1J_{CH}$ = 131.6, 130.7, and 125.5 Hz, respectively. The implications of these observed coupling constants concerning the bonding of the benzyl group to the metal center are discussed later. For now, it is sufficient to note that the above features clearly establish that the two methylene carbon environments are very different at low temperatures.

Furthermore, the low-temperature solution gated decoupled and attached proton test (APT) ^{13}C NMR experiments can be used to determine the chemical shifts of the signals due to the two ipso carbon atoms of the bis(benzyl) complexes. Consider, for instance, the relevant spectra for complex **1b** presented in Figure 3c,d. The carbon resonance at 149.2 ppm is thus assigned to the ipso carbon of the η^1-CH_2Ph' ligand, and the other resonances in the region δ 143–148 ppm are assigned to the other phenyl carbon atoms of the $CH_2C_6H_2\text{-}2,4,6\text{-}Me_3$ ligands. The chemical shift of the signal due to the ipso carbon of the η^1-CH_2Ph' ligand in each of the other bis(benzyl) complexes is at approximately 152 ppm and appears to be insensitive to the nature of the Cp′M(NO) group. On the other hand, the resonance due to the ipso carbon of the η^2-CH_2Ph' ligand in the bis(benzyl) complexes occurs upfield in the region δ 115–104 ppm, and its chemical shift is quite dependent on the nature of the Cp′M(NO) fragment to which it is attached (see Table II).

The ^{13}C CP/MAS solid-state NMR spectra of the bis(benzyl) complexes **1a**, **1b**, **2**, **3**, and **4** were recorded at ambient temperatures by Drs. C. A. Fyfe and H. Gies of this department. The similarity of these spectra with the corresponding low-temperature $^{13}C\{^1H\}$ solution NMR spectra establishes unambiguously that the molecular structure of the low-temperature form of each of the bis(benzyl) complexes in CD_2Cl_2 solutions is identical with its solid-state molecular structure. Again, the spectra obtained for complex **1a** provide a representative example. The low-temperature 25-MHz $^{13}C\{^1H\}$ NMR spectrum of **1a** in CD_2Cl_2 solution and its ^{13}C CP/MAS solid-state NMR spectrum at ambient temperature are displayed in Figure 5 for comparison. Clearly, the two spectra are very similar. Most important is the correspondence of the chemical shifts of the two ipso carbon resonances and the methylene carbon resonances in the two spectra.

Determination of the Free Energies of Activation for the Fluxional Processes. A series of ^1H NMR spectra at various temperatures can be obtained for each of the bis(benzyl) complexes, a portion of those recorded for complex **1a** being shown in Figure 6 as a representative example. Each complex exhibits coalescence of the methylene proton resonances at some well-defined temperature (see Table VII). The free energy of activation, ΔG^{*}, for the fluxional process of each bis(benzyl) complex may be determined from the temperature for coalescence, T_c, and the difference in the chemical shift ($\Delta\nu_c$ in Hz) between the methylene proton signals undergoing coales-

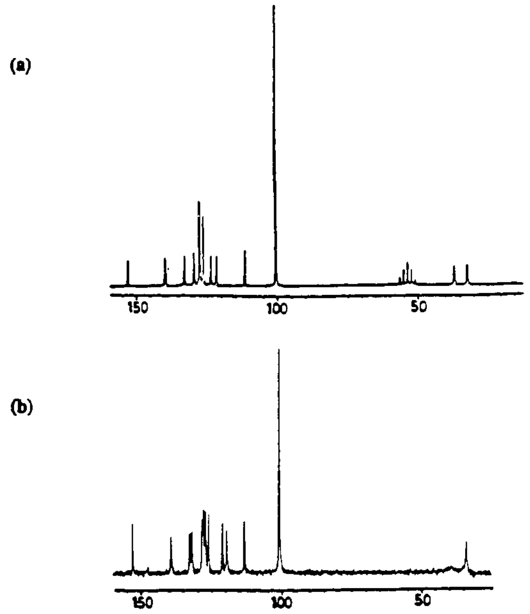

Figure 5. (a) 75-MHz $^{13}C\{^1H\}$ NMR spectrum of CpMo(NO)-$(CH_2Ph)_2$ (**1a**) in CD_2Cl_2 solution at 193 K and (b) 100-MHz ^{13}C CP/MAS NMR spectrum of CpMo(NO)$(CH_2Ph)_2$ (**1a**) at ambient temperature.

Table VII. Parameters Characterizing the Fluxional Processes Exhibited by the Bis(benzyl) Nitrosyl Complexes

complex	T_c, K	$\Delta G^*(\nu_{1,3})$, kcal/mol	$\Delta G^*(\nu_{2,4})$, kcal/mol
CpMo(NO)$(CH_2C_6H_2\text{-}2,4,6\text{-}Me_3)_2$	266 (4)	12.0 (2)	11.2 (2)
CpMo(NO)$(CH_2Ph)_2$	232 (3)	10.9 (3)	10.5 (3)
Cp*Mo(NO)$(CH_2Ph)_2$	203 (3)	9.3 (3)	9.1 (3)
CpW(NO)$(CH_2Ph)_2$	210 (3)	9.8 (3)	9.5 (3)
Cp*W(NO)$(CH_2Ph)_2$	183 (5)	8.4 (5)	8.2 (5)

cence at T_c by employing the following equation (K_B being the Boltzmann constant):[32]

$$\Delta G^* = -RT_c \ln \left[(\pi h/\sqrt{2}K_B)(\Delta\nu_c/T_c)\right]$$

The values for $\Delta\nu_c$ (i.e. $\Delta\nu_{(1,3)c}$ and $\Delta\nu_{(2,4)c}$), which correspond to the difference in chemical shift for the halves of the AB and AX methylene patterns observed in the low-temperature spectrum, were estimated according to the method outlined by Fryzuk and MacNeil.[33] The same coalescence temperature, T_c, was used for both $\Delta\nu_{(1,3)c}$ and $\Delta\nu_{(2,4)c}$,[34] and thus two values for ΔG^* were calculated for each complex. The average ΔG^* value determined for each compound (Table VII) indicates that the fluxional processes are very facile in solution at low temperature. Furthermore, an interesting trend is evident from the data presented in Table VII. The temperature of coalescence varies dramatically (as much as 83 K) depending on the Cp′M(NO) fragment to which the benzyl ligands are attached. The molybdenum bis(benzyl) complexes exhibit coalescence at higher temperatures than do their tungsten analogues. The results clearly indicate that the fluxional processes at low temperature are much more facile for the tungsten bis(benzyl) complexes than for those of molybdenum. It can thus be assumed with some confidence that at room temperature the tungsten bis(benzyl) complexes are also more fluxional than are their molybdenum analogues.

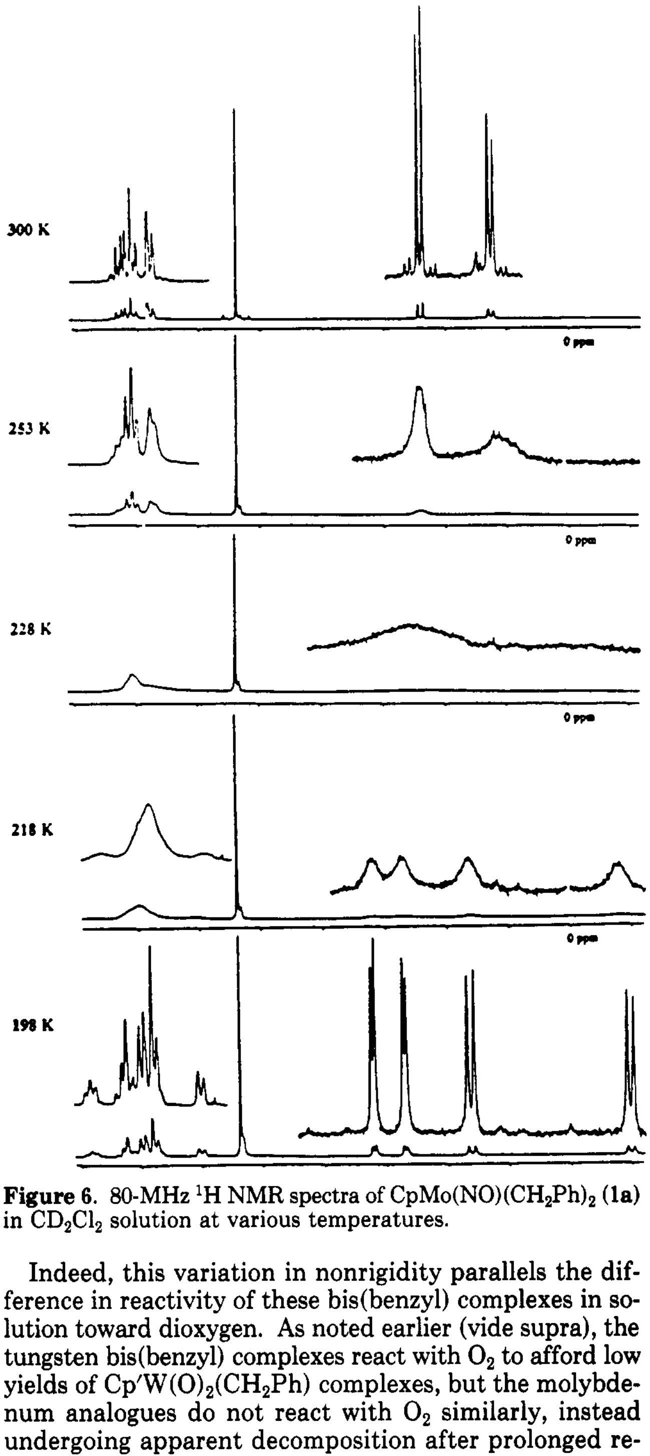

Figure 6. 80-MHz ^1H NMR spectra of CpMo(NO)$(CH_2Ph)_2$ (**1a**) in CD_2Cl_2 solution at various temperatures.

Indeed, this variation in nonrigidity parallels the difference in reactivity of these bis(benzyl) complexes in solution toward dioxygen. As noted earlier (vide supra), the tungsten bis(benzyl) complexes react with O_2 to afford low yields of Cp′W$(O)_2(CH_2Ph)$ complexes, but the molybdenum analogues do not react with O_2 similarly, instead undergoing apparent decomposition after prolonged reaction times. If the mechanism diagrammed for these types of reactions in the Introduction is indeed operative, the rate of the reactions will be governed by the ease with which the dioxygen molecule can approach the metal center. These 18-electron bis(benzyl) complexes are sterically more congested about the molybdenum or tungsten centers than are their 16-electron dialkyl analogues, Cp′M(NO)R_2 (R = Me, CH_2SiMe_3, CH_2CMe_3, and CH_2CMe_2Ph), a fact that explains qualitatively why they are inert to O_2 as solids and why they show limited reactivity in solution.

The fact that the metal center in the bis(benzyl) complexes is indeed somewhat protected from incoming Lewis bases is manifested by the difference in the reactivity of the Cp′W(NO)$(CH_2Ph)_2$ and Cp′W(NO)$(CH_2SiMe_3)_2$ complexes with alcohols as determined by NMR spectroscopy (see Experimental Section). Reaction of Cp*W-

---

[32] Thomas, W. A. *Annu. Rev. NMR Spectrosc.* **1968**, *1*, 43.

[33] Fryzuk, M. D.; MacNeil, P. *J. Am. Chem. Soc.* **1984**, *106*, 6993.

[34] Since these two sets of methylene protons do not coalesce at precisely the same temperature, the calculated values of ΔG^* are not identical.

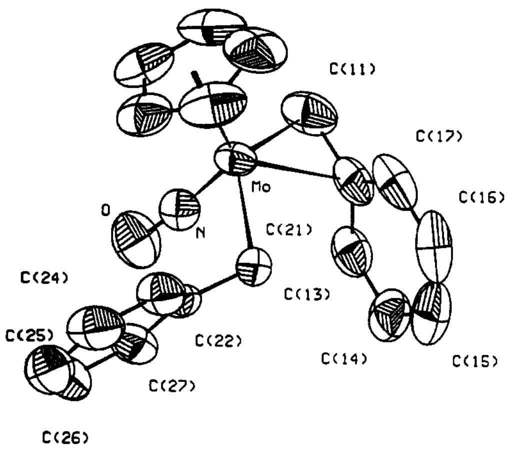

Figure 7. View of the solid-state molecular structure of $CpMo(NO)(CH_2Ph)_2$ (**1a**). Hydrogen atoms have been omitted.

$(NO)(CH_2SiMe_3)_2$ with MeOH to form $Cp^*W(NO)(OMe)(CH_2SiMe_3)$ occurs rapidly (i.e. 1–3 h at 20 °C), while the analogous reaction of $Cp^*W(NO)(CH_2Ph)_2$ with MeOH to form $Cp^*W(NO)(OMe)(CH_2Ph)$ requires many weeks at room temperature to reach completion. Furthermore, reaction of $CpW(NO)(CH_2SiMe_3)_2$ with *t*-BuOH at ambient temperature affords $CpW(NO)(O\text{-}t\text{-}Bu)(CH_2SiMe_3)$ over the course of several days, but no reaction of $CpW(NO)(CH_2Ph)_2$ with *t*-BuOH is apparent even after 6 months.

X-ray Crystallographic Analyses of the Complexes 1a, 1b, 2, 3, and 4. The single-crystal X-ray crystallographic analysis of $CpMo(NO)(CH_2Ph)_2$ (**1a**), the essential details of which are summarized in Table III, has established that this organometallic complex is not a coordinatively unsaturated compound as are its $CpM(NO)R_2$ analogues (R = CH_2SiMe_3, CH_2CMe_3, and CH_2CMe_2Ph).[35] Replacement of these alkyl groups of the $CpM(NO)R_2$ complexes with an alkyl ligand that may provide additional electron density to the metal center (such as CH_2Ph) permits the metal to accept this extra electron density in order to attain the more stable 18-electron configuration. As can be seen in the thermal ellipsoid plot shown in Figure 7, the bis(benzyl) complex **1a** possesses a pseudo four-legged piano-stool molecular structure that contains an essentially linear nitrosyl ligand (Mo–N–O angle of 174.1 (3)°), a "normal" η^1-CH_2Ph ligand, and a second benzyl ligand bonded to the molybdenum atom in an η^2 fashion. The pertinent intramolecular dimensions for **1a** are listed in Tables V and VI. The ligands constituting the legs of the piano stool are bent down in the customary manner from the plane parallel to the plane of the Cp ligand, with three of the legs being essentially at right angles with respect to each other, i.e. C(11)–Mo–N = 91.3 (2)° and C(21)–Mo–N = 91.2 (2)°. The η^1-CH_2Ph group is attached to the Mo atom by a normal Mo–C single bond [Mo–C(21) = 2.251 (3) Å],[1] the geometry around the methylene carbon atom, C(21), being essentially tetrahedral (e.g. Mo–C(21)–C(22) = 114.4°) and reflective of its sp^3 hybridization. The unique η^2-CH_2Ph ligand in **1a** involves bonding of only its methylene and ipso carbon atoms to the Mo center. Its Mo–CH_2 bond length of 2.203 (4) Å is significantly shorter than the Mo–CH_2 distance involving the η^1-CH_2Ph ligand and is indicative of the existence of a strong bonding interaction between the methylene carbon of the η^2-benzyl group and the central Mo atom. The Mo–C_{ipso} bond length of 2.433 (3) Å is indicative of the presence of a Mo–C single bond.[1] The two Mo–C_{ortho} distances of 2.808 (5) and 3.236 (4) Å, however, are much longer than those typically found for normal Mo–C bonds.[1] These latter two distances, being inequivalent, establish that the η^2-benzyl ligand is slightly twisted with respect to the central Mo atom. Nevertheless, all the carbon atoms within each of the two benzyl ligands are essentially coplanar.

With a view to elucidating the effects, if any, of steric and electronic factors on the mode of linkage of the η^2-benzyl ligand in **1a**, single-crystal X-ray crystallographic analyses have also been performed on the complexes $CpMo(NO)(CH_2C_6H_2\text{-}2,4,6\text{-}Me_3)_2$ (**1b**) and $Cp^*Mo(NO)(CH_2Ph)_2$ (**2**). Table III contains a summary of the relevant experimental and crystallographic details. Views of the solid-state molecular structures of complexes **1b** and **2** are presented in Figures 8 and 9, respectively. Furthermore, with a view to perhaps gaining some insight into the differences in the reactivity observed for the *tungsten* versus the *molybdenum* bis(benzyl) complexes with molecular oxygen, crystal structure determinations were performed on the corresponding tungsten bis(benzyl) complexes, $CpW(NO)(CH_2Ph)_2$ (**3**) and $Cp^*W(NO)(CH_2Ph)_2$ (**4**). Views of their solid-state molecular structures are shown in Figures 10 and 11, respectively.

Inspection of Figures 7–11 reveals that all the bis(benzyl) nitrosyl complexes prepared during this work are basically isostructural, even though some of them crystallize in different space groups (Table III). The final fractional positional and isotropic thermal parameters ($U_{eq} \times 10^3$, Å^2) for the non-hydrogen atoms of each bis(benzyl) complex are provided in Table IV. The intramolecular bond lengths and bond angles for the five complexes **1a**, **1b**, **2**, **3**, and **4** are collected in Tables V and VI. These intramolecular geometrical parameters confirm that the five compounds are all representable by the general formula $Cp'M(NO)(\eta^2\text{-}CH_2Ph')(\eta^1\text{-}CH_2Ph')$ and have the basic molecular structure

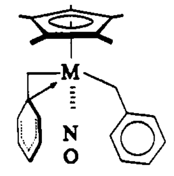

As was evident in the molecular structure of **1a** (vide supra), three of the four legs in the piano-stool structures exhibited by **1b**, **2**, **3**, and **4** are essentially at right angles to each other. In other words, the bond angles C(11)–M–N and C(21)–M–N remain near 90° in going from **1a** to **4**. The nitrosyl ligand in each structure is essentially linear, the smallest M–N–O angle being the 166.5° in **1b**. This greater bending of the M–N–O linkage in this compound is probably due to both greater M–NO back-bonding (consistent with the $CH_2C_6H_2\text{-}2,4,6\text{-}Me_3$ ligand being a better donor of σ-electron density than CH_2Ph) and steric interactions to some extent of the NO ligand with the two triply substituted phenyl rings. The η^1-benzyl ligand in each of the complexes is normal, exhibiting a M–CH_2 single bond length between 2.22 and 2.26 Å and a pseudotetrahedral environment around its methylene carbon atom. The most chemically interesting feature of each structure involves the η^2-benzyl ligand, which is characterized by the following six distinctive parameters: (a) its M–CH_2 bond length is significantly shorter (i.e. by 0.04–0.06 Å) than that involving the η^1-CH_2Ph group; (b) its CH_2–C_{ipso} bond length is also significantly shorter than that seen for the η^1-CH_2Ph group; for instance, C(11)–C(12) = 1.445 (6) and 1.457 (6) Å and C(21)–C(22) = 1.472 (4) and 1.497 (5) Å

---

(35) Legzdins, P.; Rettig, S. J.; Sánchez, L. *Organometallics* **1985**, *4*, 1470.

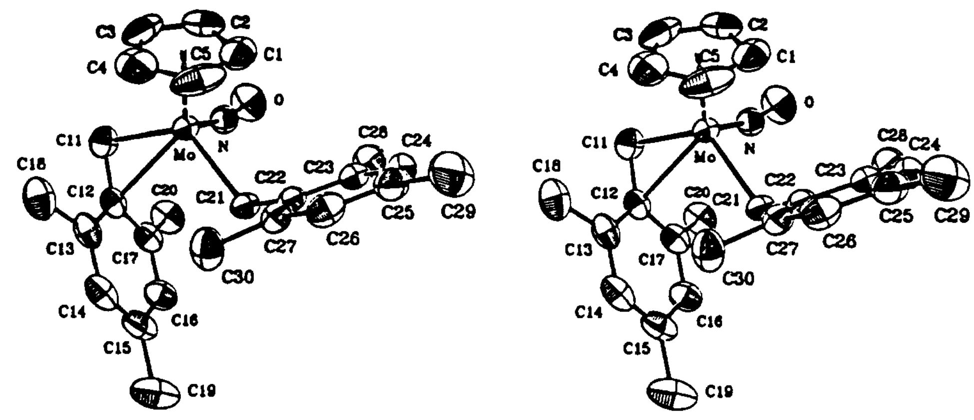

Figure 8. Stereoview of the solid-state molecular structure of $CpMo(NO)(CH_2C_6H_2\text{-}2,4,6\text{-}Me_3)_2$ (**1b**). Hydrogen atoms have been omitted.

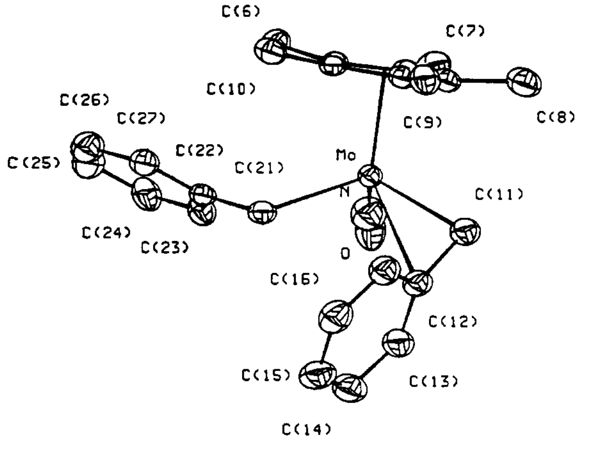

Figure 9. View of the solid-state molecular structure of $Cp^*Mo(NO)(CH_2Ph)_2$ (**2**). Hydrogen atoms have been omitted.

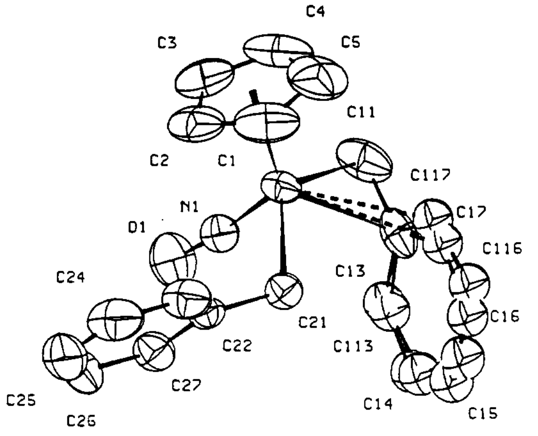

Figure 10. View of the solid-state molecular structure of $CpW(NO)(CH_2Ph)_2$ (**3**). Hydrogen atoms have been omitted.

in complexes **1a** and **2**, respectively; (c) its $M\text{-}C_{ipso}$ distance (ranging between 2.433 (6) and 2.510 (4) Å) is well within the range expected for a normal group 6 metal-carbon single bond; (d) its angle at the methylene carbon atom (i.e. C(12)-C(11)-M) is well below the value expected for a tetrahedral sp^3 carbon environment, being typically in the range 81-85°; (e) its two $M\text{-}C_{ortho}$ distances (ranging between 2.81 and 3.26 Å) are longer than the range commonly observed for strong group 6 M-C single bonds; and (f) its four phenyl C-C distances from C(13) to C(17) are essentially identical, and the observed bond lengths of approximately 1.38 Å suggest the presence of delocalized multiple bonding extending over these carbons.

These metrical parameters closely resemble those found for the η^2-benzyl ligand in $Cp^*Mo(NO)(CH_2SiMe_3)(\eta^2\text{-}CH_2Ph)$.[1] Consequently, we formulate the bonding in the metal-η^2-benzyl linkages of the five bis(benzyl) complexes in an analogous manner, i.e.

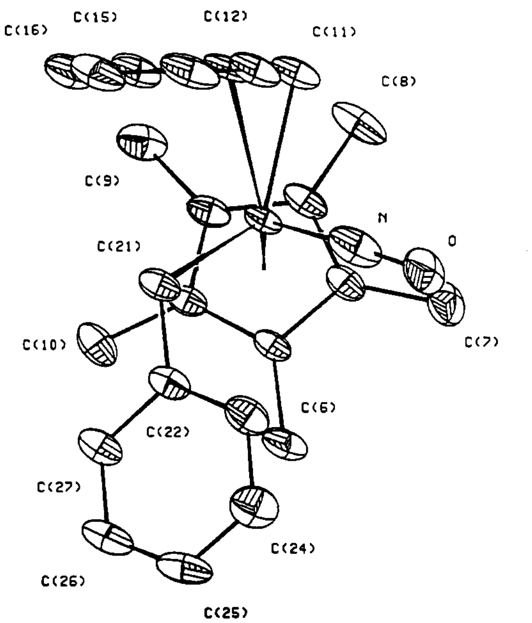

Figure 11. View of the solid-state molecular structure of $Cp^*W(NO)(CH_2Ph)_2$ (**4**) showing the planarity of the η^2-CH_2Ph ring with respect to the central tungsten atom. Hydrogen atoms have been omitted.

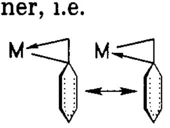

This representation of the metal-benzyl interactions by the resonance hybrid shown above thus indicates that two electrons have been removed from the phenyl ring's π system and are being provided to the metal center via a carbon-to-metal σ donor bond. This bond, combined with the other, normal C-M σ covalent bond shown in either limiting form of the resonance hybrid above, thus enables the η^2-benzyl ligands to function as formal three-electron donors and permits the metal centers to attain the favored 18-valence-electron configurations. Hence, all five bis(benzyl) nitrosyl complexes are diamagnetic, a conclusion fully supported by their ^1H and ^{13}C NMR spectroscopic properties (vide supra). These properties also are consistent with the bonding of the benzyl group to the metal center presented above. Thus, the low-temperature gated decoupled ^{13}C NMR spectra establish that the methylene carbon atoms of the η^2-benzyl groups are primarily sp^2 in character[36] ($^1J_{CH}$ = 152-148 Hz as compared to $^1J_{CH}$ =

Table VIII. Comparison of the Intramolecular Dimensions in Structurally Characterized Metal–Benzyl Complexes[a]

	distance, Å						
complex	$\mathrm{M{-}CH_2}$[b]	$\mathrm{M{-}C_{ipso}}$[c]	$\mathrm{M{-}C_{ortho}}$[d]	$\mathrm{M{-}C_{ortho'}}$[e]	Δ[f]	Δ[g]	ref
			Late Transition Metals				
$\mathrm{Ni(\eta^3\text{-}CH_2C_6H_4\text{-}\mathit{o}\text{-}Me)Cl_2(PMe_3)}$	1.930	2.050	2.318	*h*	0.12	large	37
$\mathrm{Pt(\eta^3\text{-}CPh_3)(acac)}$	2.088	2.120	2.148	3.081	0.028	0.96	38c
$\mathrm{Pd(\eta^3\text{-}CPh_3)(acac)}$	2.105	2.154	2.200	3.132	0.046	0.998	38c
$\mathrm{Co(\eta^3\text{-}CH_2Ph)[P(OMe)_3]_3}$	2.036	2.117	2.408	*h*	0.029	large	38d
$\mathrm{Rh(\eta^3\text{-}CH_2C_6Me_5)[P(O\text{-}\mathit{i}\text{-}Pr)_3]_2}$	2.128	2.246	2.453	*h*	0.21	large	38e
			Middle Transition Metals				
$\mathrm{Fe_2(DPF)(CO)_5}$[i]	2.11	2.16	2.22	*h*	0.067	large	38b
$\mathrm{Ru_2(DPF)(CO)_5}$[i]	2.24	2.32	2.34	*h*	0.019	large	38b
$\mathrm{Mo(\eta^3\text{-}CH_2Ph\text{-}\mathit{p}\text{-}Me)Cp(CO)_2}$	2.27	2.36	2.48	3.31	0.115	0.945	38a
$\mathrm{Mo(\eta^2\text{-}CH_2Ph)(\eta^1\text{-}CH_2Ph)Cp(NO)}$	2.203	2.433	2.808	3.236	0.375	0.803	*j*
$\mathrm{Mo(\eta^2\text{-}CH_2Ph')(\eta^1\text{-}CH_2Ph')Cp(NO)}$	2.196	2.483	3.101	3.172	0.618	0.689	*j*
$\mathrm{Mo(\eta^2\text{-}CH_2Ph)(\eta^1\text{-}CH_2Ph)Cp^*(NO)}$	2.191	2.493	2.949	3.250	0.456	0.757	*j*
$\mathrm{W(\eta^2\text{-}CH_2Ph)(\eta^1\text{-}CH_2Ph)Cp(NO)}$	2.179	2.444	2.938	3.209	0.494	0.765	*j*
$\mathrm{W(\eta^2\text{-}CH_2Ph)(\eta^1\text{-}CH_2Ph)Cp^*(NO)}$	2.173	2.510	3.015	3.261	0.505	0.751	*j*
$\mathrm{Mo(\eta^2\text{-}CH_2Ph)(CH_2SiMe_3)Cp^*(NO)}$	2.188	2.473	3.004	3.234	0.531	0.761	1
			Early Transition/Actinide Metals				
$\mathrm{[Zr(\eta^2\text{-}CH_2Ph)Cp_2(N{\equiv}CCH_3)]^+}$	2.344	2.648	3.236	3.25	0.59	0.60	40
$\mathrm{Th(CH_2Ph)_3Cp^*}$	2.579	2.865	3.352	3.574	0.48	0.71	39d
$\mathrm{Th(CH_2Ph)_4(dmpe)}$[k]	2.53	2.86	3.31	3.44	0.43	0.58	39e
$\mathrm{U(CH_2Ph)_3Me(dmpe)}$[k]	2.54	2.758	3.089	3.450	0.33	0.69	39e

[a] The data listed are with respect to the η^n-benzyl group (n = 2–4) in each of the complexes. [b] The metal to methylene carbon bond length. [c] The metal to ipso carbon bond length. [d] The shortest metal to ortho carbon bond length or distance. [e] The longest metal to ortho carbon bond length or distance. [f] $[(\mathrm{M{-}C_{ortho}}) - (\mathrm{M{-}CH_2})] - [(\mathrm{M{-}C_{ipso}}) - (\mathrm{M{-}CH_2})]$. [g] $[(\mathrm{M{-}C_{ortho'}}) - (\mathrm{M{-}CH_2})] - [(\mathrm{M{-}C_{ipso}}) - (\mathrm{M{-}CH_2})]$. [h] This bond distance was not reported (but can be calculated from the atomic fractional coordinates reported for the complex). [i] DPF = μ-η^3,η^5-$\mathrm{C(C_6H_5)_2(C_5H_4)}$. [j] This work. [k] dmpe = $\mathrm{Me_2PCH_2CH_2PMe_2}$.

131.6–125 Hz for the normal η^1-benzyl ligand). Furthermore, the ^{13}C NMR spectroscopic data (both CP/MAS and low-temperature solution) indicate the existence of a strong interaction between the ipso carbon atom of the η^2-benzyl ligand and the metal center. The chemical shifts of these carbons' resonances occur in the spectral range δ 115–104 ppm, a range considerably upfield from where resonances for aromatic quaternary carbon atoms are typically observed (i.e. δ 160–145 ppm).[36]

Comparisons of the Intramolecular Dimensions in Structurally Characterized Metal–Benzyl Linkages. To date, five different types of metal–benzyl linkages have been reported in the literature:[1,37]

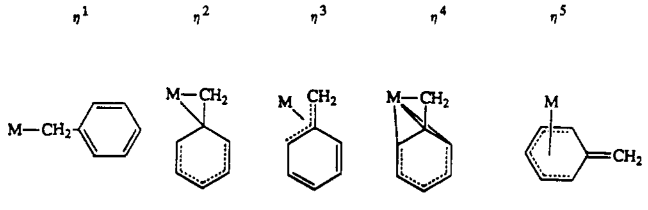

Some of these cases have also been authenticated by X-ray crystallography.[1,37] As noted by other investigators,[37] the adoption of a particular coordination mode by the benzyl-type ligand is strongly dependent on the nature of the ML_n fragment to which it is bonded. To put the structural studies presented in this paper in their proper context, it is instructive to compare the intramolecular dimensions of the η^2-benzyl ligands in complexes **1a**, **1b**, **2**, **3**, and **4** to those of other structurally characterized metal–η^2-benzyl, –η^3-benzyl, and –η^4-benzyl linkages reported in the literature. Such a comparison might provide some clue as to why the benzyl ligand attachments vary from one class of complexes to another and how these variations may be reflected in differing reactivities of the bound benzyl ligands. The most informative comparisons involve the metal to methylene carbon, metal to ipso carbon, and metal to ortho carbon bond lengths. These distances, determined in our and several other structurally characterized η^n-benzyl-containing (n = 2–4) complexes, are collected in Table VIII in a manner first used by Zalkin et al.[38,39e] to permit ready comparisons of the structural parameters.

In all the η^3-benzyl complexes listed at the top of Table VIII, the benzyl group is bound to the metal in an unsymmetrical fashion, the metal–carbon bond lengths increasing in the order $\mathrm{M{-}CH_2} < \mathrm{M{-}C_{ipso}} < \mathrm{M{-}C_{ortho}}$. The $\mathrm{M{-}CH_2}$ and $\mathrm{M{-}C_{ipso}}$ bond lengths are usually similar in length, being at least to within 0.03–0.12 Å of each other. The $\mathrm{M{-}C_{ortho}}$ bond lengths, on the other hand, exhibit much greater variation, distances between 2.1 and 2.5 Å being typical. Interestingly, the $\mathrm{M{-}C_{ipso}}$ bond lengths in **1a**, **1b**, **2**, **3**, and **4** are similar in magnitude to the $\mathrm{M{-}C_{ortho}}$ bond lengths in typical η^3-benzyl complexes. The closest metal to ortho carbon distances in **1a**, **1b**, **2**, **3**, and **4** are approximately 2.8–3.1 Å. The difference between the $\mathrm{M{-}C_{ortho}}$ bond length and the $\mathrm{M{-}CH_2}$ bond length, $[(\mathrm{M{-}C_{ortho}}) - (\mathrm{M{-}CH_2})]$, in the η^3-benzyl complexes typically lies within the range 0.1–0.4 Å. This contrasts with the range 0.6–0.9 Å for $[(\mathrm{M{-}C_{ortho}}) - (\mathrm{M{-}CH_2})]$ in **1a**, **1b**, **2**, **3**, and **4**. This comparison clearly establishes the structural

---

(36) (a) Levy, G. C.; Lichter, R. L.; Nelson, G. L. *Carbon-13 Nuclear Magnetic Resonance Spectroscopy*, 2nd ed.; John Wiley and Sons: New York, 1980. (b) Mann, B. E.; Taylor, B. F. *^{13}C NMR Data for Organometallic Compounds*; Academic Press: London, 1981. (c) Becker, E. B. *High Resolution NMR: Theory and Chemical Applications*, 2nd ed.; Academic Press: New York, 1980.

(37) Carmona, E.; Marin, J. M.; Paneque, M.; Poveda, M. L. *Organometallics* **1987**, *6*, 1757 and references cited therein.

(38) (a) Cotton, F. A.; LaPrade, M. D. *J. Am. Chem. Soc.* **1968**, *90*, 5418. (b) Behrens, U.; Weiss, E. *J. Organomet. Chem.* **1975**, *96*, 399, 435. (c) Bailey, P. M.; Maitlis, P. M.; Sonoda, A. *J. Chem. Soc., Dalton Trans.* 1979, 346. (d) Bleeke, J. R.; Burch, R. R.; Coulman, C. L.; Schardt, B. C. *Inorg. Chem.* **1981**, *20*, 1316. (e) Burch, R. R.; Muetterties, E. L.; Day, V. W. *Organometallics* **1982**, *1*, 188.

(39) (a) Bassi, I. W.; Allegra, G.; Scordamaglia, R.; Chioccola, G. *J. Am. Chem. Soc.* **1971**, *93*, 3787. (b) Davies, G. R.; Jarvis, J. A. J.; Kilbourn, B. T.; Pioli, A. J. P. *J. Chem. Soc., Chem. Commun.* **1971**, 677. (c) Davies, G. R.; Jarvis, J. A. J.; Kilbourn, B. T. *J. Chem. Soc., Chem. Commun.* 1971, 1511. (d) Mintz, E. A.; Moloy, K. G.; Marks, T. J.; Day, V. W. *J. Am. Chem. Soc.* **1982**, *104*, 4692. (e) Edwards, P. G.; Anderson, R. A.; Zalkin, A. *Organometallics* **1984**, *3*, 293.

(40) Jordan, R. F.; LaPointe, R. E.; Baenziger, N.; Hinch, G. D. *Organometallics* **1990**, *9*, 1539 and references cited therein.

difference between the bis(benzyl) complexes prepared in this work and typical η^3-benzyl complexes described in the literature. The metal to nonbonding ortho carbon distance in η^3-benzyl complexes is always longer than 3.0 Å, the difference [(M–C$_{ortho'}$) – (M–CH$_2$)] being close to or greater than 1.0 Å. The large difference between the two values Δ and Δ' in Table VIII for the η^3-benzyl complexes is indicative of the "edge-on" mode of attachment of the benzyl ligand. In complexes **1a**, **1b**, **2**, **3**, and **4**, however, these two values are nearly equivalent, a feature reflective of the "face-on" mode of attachment of the η^2-benzyl ligands in these cases. Also, in virtually all the structurally characterized η^3-benzyl complexes, the expected carbon–carbon bond length alternation is observed in the aromatic ring of the benzyl group. The arene ring π-delocalization is disrupted to such an extent that the ring dimensions approach those of a *cis*-1,3-butadiene group, which has a C—C single-bond length of 1.47 Å and C═C double-bond lengths of approximately 1.34 Å. As noted above, the C–C bond lengths in the η^2-benzyl ligand in each of the complexes **1a**, **1b**, **2**, **3**, and **4** do not exhibit this alternation in length. Instead, the two C–C bond lengths within the ring of the η^2-benzyl ligand, i.e. C(12)–C(13) and C(12)–C(17), are slightly longer (ca. 1.39–1.42 Å) than the other four C–C bond lengths [C(13)–C(14), C(14)–C(15), C(15)–C(16), and C(16)–C(17)], which are all approximately equal (ca. 1.35–1.39 Å), thereby suggesting almost normal arene delocalization in most of the ring.

Replacement of the two carbonyl ligands in the complex CpMo(CO)$_2$(η^3-CH$_2$C$_6$H$_4$-*p*-Me) with a nitrosyl group and an alkyl ligand (in this case another benzyl group) to give the formally valence-isoelectronic complex **1a** results in a clearly different mode of binding of the benzyl group to the molybdenum center. This fact is interesting in light of what might have been expected on the basis of electronic arguments. The presence of the nitrosyl ligand (a stronger electron-withdrawing group than the CO ligand) would be expected to result in the molybdenum metal center in **1a** exhibiting a more electrophilic character than in CpMo(CO)$_2$(η^3-CH$_2$C$_6$H$_4$-*p*-Me). As a result, a larger interaction of the molybdenum's empty d orbitals with the electron density on the arene ring of the benzyl ligand might have been anticipated for **1a**. However, the closest Mo–C$_{ortho}$ distance in **1a** (2.808 Å) is approximately 0.33 Å longer than the Mo–C$_{ortho}$ bond length (2.48 Å) in the η^3-benzyl ligand of CpMo(CO)$_2$(η^3-CH$_2$C$_6$H$_4$-*p*-Me). In fact, the closest Mo–C$_{ortho}$ distance in **1a** is 0.40 Å longer than the corresponding M–C$_{ortho}$ bond length in the most unsymmetrical η^3-benzyl complex known, namely Co(η^3-CH$_2$Ph)[P(OEt)$_3$]$_3$.[38d] In a similar fashion, all the M–C$_{ortho}$ distances in complexes **1b**, **2**, **3**, and **4** are much longer than the typical M–C$_{ortho}$ bond lengths extant in η^3-benzyl complexes (Table VIII).

The intramolecular dimensions of the η^2-benzyl ligands in each of the structures **1a**, **1b**, **2**, **3**, and **4** resemble those determined for other η^2- or η^4-benzyl complexes of early transition or actinide metals (Table VIII). Some of the M–C$_{ipso}$ bond lengths in these early-metal benzyl complexes are short enough to be consistent with the existence of M–C single bonds (i.e. [(M–C$_{ipso}$) – (M–CH$_2$)] = 0.22–0.35 Å). However, the true nature of the bonding of some of the benzyl groups in these early-metal complexes is somewhat ambiguous. For instance, the M–C$_{ortho}$ distances in the η^4-benzyl–metal linkages are often longer than expected, and the differences in bond lengths [(M–C$_{ortho}$) – (M–CH$_2$)] and [(M–C$_{ortho}$) – (M–C$_{ipso}$)] usually range between 0.55–0.90 and 0.3–0.6 Å, respectively. Unlike the η^3-benzyl complexes listed in Table VIII, the two values Δ and Δ' are nearly equivalent in each of these early transition/actinide metal benzyl complexes, as they are in **1a**, **1b**, **2**, **3**, and **4**. This equivalence is simply a manifestation of the benzyl ligand being planar with respect to the central metal atom. Hence, it is clear that theoretical calculations are needed to determine precisely the orbitals involved in the bonding of these unusual η^2- and η^4-benzyl linkages and to establish whether indeed they are quantitatively different.

A comparison of the intramolecular dimensions in each of the complexes **1a**, **1b**, **2**, **3**, and **4** reveals subtle variations in the linkage of the η^2-benzyl fragment depending on Cp versus Cp*, Ph versus Ph′, and Mo versus W. The changes in the attachment of the benzyl group to the metal center are not always statistically significant in going from one complex to the next, but some trends are evident in going from structures **1a** to **4**. For instance, the differences between the M–C$_{ipso}$ and M–CH$_2$ bond lengths, [(M–C$_{ipso}$) – (M–CH$_2$)], and the M–C$_{ortho}$ and M–CH$_2$ bond lengths, [(M–C$_{ortho}$) – (M–CH$_2$)], and the sizes of the bond angles C(12)–C(11)–M and C(17)–C(12)–M increase as the Cp ligand is replaced by a Cp* group and the central metal atom is changed from Mo to W. These changes in the intramolecular dimensions are consistent with the benzyl group moving away from the metal atom at the ipso carbon. As a result of the η^2-benzyl ligand backing away from the metal center, the angle between the nitrosyl ligand and the normal η^1-benzyl group increases slightly (e.g., the angles C(21)–M–N for **1a**, **1b**, **2**, **3**, and **4** are 91.2, 94.8, 92.9, 91.7, and 94.0°, respectively). Furthermore, the two metal–ortho carbon distances of the unique η^2-benzyl ligand in each structure slowly become more similar in length in going from **1a** to **4**. For instance, the M–C$_{ortho}$ distances of 2.808 (5) and 3.236 (4) Å in **1a** lengthen to 3.015 (4) and 3.261 (4) Å in **4**, thereby indicating that as the benzyl group moves away from the central metal atom, it also slowly becomes less tilted with respect to the metal. In closing this section, it should be reiterated that all the M–C$_{ortho}$ distances are significantly longer than typical group 6 M–C single bonds, the six carbon atoms of the benzyl ligand are always coplanar, and the C–C bond lengths in the unique benzyl group do not show the characteristic alternation observed in η^3-benzyl complexes (i.e. do not approach a *cis*-1,3-butadiene structure).

Epilogue

This work has established that the Cp′M(NO)(CH$_2$Ph′)$_2$ complexes (Cp′ = Cp or Cp*; M = Mo or W; Ph′ = C$_6$H$_5$ or C$_6$H$_2$-2,4,6-Me$_3$) are unique members in the class of dialkyl cyclopentadienyl nitrosyl complexes of molybdenum and tungsten. They are formally coordinatively saturated, 18-electron species possessing unusual Cp′M(NO)(η^2-CH$_2$Ph′)(η^1-CH$_2$Ph′) molecular structures both in the solid state and in solutions at low temperatures. Variable-temperature ^{1}H and ^{13}C NMR spectroscopy of the complexes in CD$_2$Cl$_2$ solutions establishes that they are stereochemically nonrigid and undergo a facile fluxional process, the two benzyl ligands interchanging their modes of attachment to the molybdenum or tungsten metal centers. This fluxional process is much more facile for the tungsten bis(benzyl) complexes than for the molybdenum analogues. Furthermore, it parallels the difference in reactivity of these bis(benzyl) complexes with O$_2$ and is consistent with the view that, during reactions of any Cp′M(NO)R$_2$ complex with molecular oxygen, initial attack by O$_2$ at the metal center is a prerequisite for the eventual formation of Cp′M(O)$_2$R complexes.

Furthermore, it appears as though it is principally electronic factors that determine the mode of linkage of the benzyl ligand to a particular metal center, e.g. the η^2-CH_2Ph structure in **1a** versus the η^3-$CH_2C_6H_4$-*p*-Me group in its valence isoelectronic analogue, $CpMo(CO)_2(\eta^3$-$CH_2C_6H_4$-*p*-Me). On the basis of the similarities of the solid-state molecular structures possessed by complexes **1a**, **1b**, and **2**, it seems that steric effects play only a minor role in determining the mode of linkage of the unique benzyl ligand. Indeed, the propensity to attach benzyl ligands in an η^2 manner appears to be a general property of this class of compounds, since a variety of other Cp′M(NO)X(η^2-CH_2Ph) complexes (Cp′ = Cp or Cp*; M = Mo or W; X = alkyl or halide) display this structural feature.[41] Nevertheless, while the valence-bond resonance forms provided earlier in this paper represent a reasonable description of the M–η^2-benzyl bonding in complexes **1a**, **1b**, **2**, **3**, and **4**, they do not provide a rationale for why the benzyl ligands in these compounds do not coordinate in an η^3 fashion to the metal centers and undergo the characteristic σ–π electronic distortion found for the allyl ligands in the related CpW(NO)(η^3-allyl)X compounds.[42]

Acknowledgment. We are grateful to the Natural Sciences and Engineering Research Council of Canada for support of this work in the form of grants to P.L., J.T., and F.W.B.E. We also thank Drs. C. A. Fyfe and H. Gies of this department for recording the ^{13}C CP/MAS solid-state NMR spectra of the bis(benzyl) complexes **1a**, **1b**, **2**, **3**, and **4**.

Supplementary Material Available: Tables of anisotropic thermal parameters for the non-hydrogen atoms and positional and thermal parameters for the hydrogen atoms of **1a**, **1b**, **2**, **3**, and **4** and tables of bond lengths and bond angles involving the hydrogen atoms for **1a**, **1b**, **2**, and **4** (27 pages); listings of observed and calculated structure factors for all the complexes (105 pages). Ordering information is given on any current masthead page.

---

[41] Dryden, N. H.; Legzdins, P. Manuscript in preparation.

[42] Greenhough, T. J.; Legzdins, P.; Martin, D. T.; Trotter, J. *Inorg. Chem.* 1979, *18*, 3268 and references cited therein.

Thermolysis of Cp*Rh{(η^4:η^1-C_4Me_4S)Fe(CO)$_4$}: A Case Study in Thiophene Desulfurization

Shifang Luo, Ann E. Ogilvy, Thomas B. Rauchfuss,* Arnold L. Rheingold,† and Scott R. Wilson

School of Chemical Sciences, University of Illinois, Urbana, Illinois 61801,
and Department of Chemistry, University of Delaware, Newark, Delaware 19711

Received September 11, 1990

Cp*Rh(η^4-C_4Me_4S) (**1**) and $Fe_3(CO)_{12}$ react to give the ferrole Cp*Rh{η^5-$C_4Me_4Fe(CO)_3$} (**3**) together with trace amounts of Cp*Rh{(η^4:η^1-C_4Me_4S)Fe(CO)$_4$} (**2**). Compound **2** was prepared in high yield by the reaction of **1** with $Fe(CO)_5$ in the presence of Me_3NO. Thermolysis of **2** in refluxing toluene gave **3**, free C_4Me_4S (tetramethylthiophene, TMT), and $(Cp^*Rh)_2(\mu$-CO)(μ_3-S)Fe(CO)$_3$ (**4**) in ca. 2:2:1 molar ratio. The efficiency of the conversion of **2** to **3** increased with added $Fe_3(CO)_{12}$ concomitant with the diminution of the yield for **4**. Control experiments showed that **3** and **4** are stable to $Fe_3(CO)_{12}$ in refluxing toluene. Furthermore, by labeling both the rhodium, with C_5Me_4Et, and the thiophene, as C_4Me_4S-*3,4*-d_2, we showed that the Rh–C_4Me_4S moiety remains intact during its desulfurization. The structures of **2**–**4** were determined by single-crystal X-ray diffraction. The desulfurization process illustrates the following mechanistic points: (i) transition metals play a dual role in thiophene desulfurization by separately stabilizing the desulfurized hydrocarbon and accepting the sulfur, (ii) the hydrocarbon is stabilized in the form of a metallacycle that structurally resembles thiophene, and (iii) the hydrocarbon and sulfide are stabilized in heterometallic environments.

Introduction

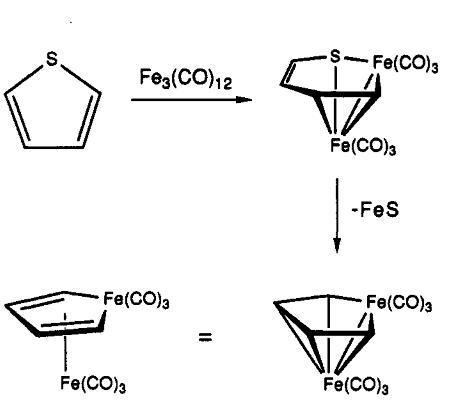

(1)

The coordination chemistry of thiophenes is of recent interest[1] because of its relevance to the metal-catalyzed hydrodesulfurization of fossil fuels.[2,3] The connection between coordination chemistry and thiophene desulfurization was first demonstrated by the research groups of Stone at Harvard and Markó at Vesprém. The former study showed that thiophene reacts with $Fe_3(CO)_{12}$ to give the ferrole $Fe_2C_4H_4(CO)_6$.[4] Subsequent work demonstrated that this reaction proceeded via thiaferroles $Fe_2SC_4R_4(CO)_6$, which convert to ferroles with the elimination of an insoluble iron sulfide (eq 1).[5] Markó and co-workers showed that thiophenes react with $Co_2(CO)_8$ to give $Co_2FeS(CO)_9$ under high pressures of hydrogen and

---

* To whom correspondence should be addressed at the University of Illinois.

† University of Delaware.

© 1991 American Chemical Society